RGNZ/MGPB

Redefining Subsidence and Uplift Hotspots on Java Island, Indonesia: Multi-Temporal InSAR for Large-Scale Land Deformation Mapping

Rudarsko-geološko-naftni zbornik
(The Mining-Geology-Petroleum Engineering Bulletin)
DOI: 10.17794/rgn.2025.4.11

Original scientific paper

Argo Galih Suhadha[1]*, Mohammad Ardha[1], Farikhotul Chusnayah[2], Rido Dwi Ismanto[3], Rizky Ahmad Yudanegara[4], Atriyon Julzarika[5]

[1] *Research Center for Geoinformatics, National Research and Innovation Agency (BRIN), Jl. Sangkuriang, Dago, Coblong, Bandung, Indonesia 40135.*

[2] *Research Center for Hydrodynamics Technology, National Research and Innovation Agency (BRIN), KST BJ. Habibie Serpong, Tangerang Selatan, 15314, Banten, Indonesia.*

[3] *Research Center for Computing, National Research and Innovation Agency (BRIN), Jl. Sangkuriang, Dago, Coblong, Bandung, Indonesia 40135.*

[4] *Department Geomatics Engineering, Institut Teknologi Sumatera, Jl. Terusan Ryacudu, Way Hui, Jatiagung, South Lampung, 35365.*

[5] *Research Center for Limnology & Water Resources, National Research & Innovation Agency (BRIN), Jl. Raya Jakarta-Bogor Km 46 Cibinong, Indonesia 16911.*

Abstract

Java Island experiences complex and nonlinear land deformation resulting from the interplay of natural and anthropogenic factors. Previous studies predominantly investigated urban subsidence, leaving island-wide patterns less understood. This research addresses that gap by utilizing Multi-Temporal Interferometric Synthetic Aperture Radar (MT-InSAR) data to identify comprehensive subsidence and uplift patterns across Java Island. MT-InSAR data reveal previously underrepresented subsidence at Karawang (-1795 mm), Cilacap (-902 mm), and Madiun (-742 mm) to be higher than coastal Jakarta's subsidence. Notably, Greater Jakarta's most severe subsidence occurs inland at Bekasi and Cikarang, which challenges common assumptions for urban subsidence. This challenges traditional perspectives on urban subsidence, offering a broader understanding of Java's regional geodynamics. By integrating hotspot analysis and MT-InSAR, the study enhances land deformation monitoring and requires continuous monitoring to enable efficient land management and infrastructure planning, particularly in high-risk, poorly monitored areas such as Karawang, Cilacap, and Madiun. These findings can be applied by geologists, urban planners, and policymakers to mitigate geological hazards and ensure sustainable development.

Keywords:
InSAR, Vertical Land Motion, LiCSBAS, land subsidence, Sentinel-1

1. Introduction

The Earth's surface continuously experiences deformation influenced by both natural processes and human activities. Uplift and subsidence form one of the most extraordinary forms of land deformation, i.e. vertical land motion (VLM). Land subsidence is becoming a growing issue along the northern coast of Java Island, the primary causes of which are groundwater over-abstraction and urbanization (**Abidin et al., 2010, 2015; Sidiq et al., 2021**). Although tectonic activity induces ground deformation in the majority of instances, its contribution to Java's subsidence is relatively negligible relative to anthropogenic subsidence (**Andreas et al., 2019**). Additionally, some areas have slope instability, which is hazardous to infrastructure, particularly roads and highways (**Saroso, 1988**).

The geological complexity of Java Island makes it prone to uneven and nonlinear deformation governed by a combination of natural geological factors and anthropogenic stressors (**Koulali et al., 2017; Malawani et al., 2020; Verstappen, 2010**). However, most research conducted on ground deformation in Indonesia has been limited to major urban areas such as Jakarta, Bandung, and Semarang, where land subsidence impacts have been extensively reported (**Abidin et al., 2013a; Khakim et al., 2013**). Small cities and peri-urban areas, whose land deformation may be equally significant, have been neglected. Such lack of understanding is limiting in planning effective mitigation strategies and is out of reach for the majority of risk-prone locations for national-scale land planning management.

Furthermore, isostasy adjustments, which govern the gravitational balance of Earth's crust, contribute to re-

* Corresponding author: Argo Galih Suhadha
e-mail address: argo003@brin.go.id

Received: 23 September 2024. Accepted: 12 March 2025.
Available online: 27 August 2025

gional land motion, where sediment deposition-induced subsidence often coincides with uplift elsewhere, as observed in post-glacial rebound and the pseudo-dynamic equilibrium along Java's northern coast (**Flament et al., 2013; Julzarika, 2024; Root et al., 2015**).

Updating unmapped or underrepresented deformation zones is crucial for accurate hazard assessments and infrastructure planning (**Li et al., 2024; Luo et al., 2022; Marsella and Scaioni, 2018**). This is particularly relevant for transport infrastructure, where precise vertical deformation data is essential for ensuring safety and maintenance (**Kalenjuk et al., 2021; Kavzoglu et al., 2009**). Studies have emphasized the importance of continuous deformation monitoring in providing early warnings of structural failures, reinforcing the need for accurate and high-resolution data (**Chrzanowski et al., 2007; Gagliardi et al., 2023**).

Traditional Global Navigation Satellite System (GNSS)-based deformation mapping, while widely used, presents limitations in spatial coverage and accuracy when monitoring large-scale vertical land motion (**Abidin et al., 2013b; Rizos Chris et al., 2000**). The GNSS method is time-consuming and costly, and it provides point data; therefore, it is inefficient for large-scale deformation tendency detection (**Meng et al., 2004**). However, since 2014, when the Sentinel-1 was introduced, Interferometric Synthetic Aperture Radar (InSAR) use has revolutionized deformation monitoring into a novel method with highly large-scale as well as high-resolution data measurement (**Cigna et al., 2019; Duan et al., 2020; Li et al., 2022; Raspini et al., 2022**). The introduction of big-data-capable SAR processing, such as multi-track geometries and satellite orbit overlaps, has contributed to InSAR's capability for monitoring long-term surface deformation (**Cigna and Tapete, 2021; Pepe and Calò, 2017; Suhadha and Harintaka, 2023, 2024**).

LiCSBAS, an open-source program for time series analysis of SAR interferometry, was recently released. It is integrated with an automated Sentinel-1 InSAR processor, COMET-LiCSAR (**Morishita et al., 2020; Thamer et al., 2023**). This platform eliminates manual preprocessing, streamlining large-scale SAR data processing while incorporating loop-closure adjustments, tropospheric corrections, and spatio-temporal filtering to ensure reliable deformation measurements across both urban and rural settings. LiCSBAS lay on the Small Baseline Subset (SBAS) method, a key component of Multi-Temporal InSAR (MT-InSAR), is particularly useful for monitoring large-scale surface deformations and has been widely employed in geodetic applications such as land subsidence, landslides, and seismic activity. Unlike Persistent Scatterer (PS) InSAR, which is best suited for detecting displacements in urban areas and on artificial structures, SBAS is capable of covering up to 85% of the observed region (**Cigna and Tapete, 2021**). It achieves this by selecting image pairs with minimal spatial and temporal separations, known as the "small baseline" approach.

Given the critical need for continuous deformation monitoring, InSAR-based observations are increasingly valuable for hazard management, early warning systems, and infrastructure planning (**Suhadha et al., 2023a, 2021; Suhadha and Julzarika, 2022**). This study employs MT-InSAR, specifically SBAS, to produce vertical displacement maps across Java Island to demarcate and categorize deformation hotspots. Unlike traditional GNSS-based approaches, MT-InSAR enables broad spatial coverage, revealing subsidence and uplift trends in large urban agglomerations such as Greater Jakarta, Bandung, and Semarang, as well as lesser-known smaller cities such as Madiun and Cilacap. In addition, GNSS data verify recently identified uplift and subsidence hotspots, increasing deformation mapping quality with InSAR.

2. Regional setting

Java Island, within Indonesia between Bali and Sumatra in the Sunda Arc, varies between approximately 5° to 8° south latitude and 105° to 115° east longitude. It covers only 7% of Indonesia's land area but holds 56% of its population. Thus, it is very susceptible to geohazards like land deformation, earthquakes, and volcanism (**Cummins, 2017**). The diverse island landscapes are created by contrasting geological processes, with tectonic and volcanic processes defining the south and other depositional environments defining the north (**Negara et al., 2021**). These variations have led to unequal watershed development, with the north undergoing more rapid land-use and land-cover changes (**Kaswanto and Utami, 2016**). Furthermore, the Tertiary and Quaternary volcanic formations of East Java have contributed to the island's unique geomorphological features (**Verstappen, 2010**). The active fault systems from the eastern to the southern Java further complicate the region's geological evolution (**Supendi et al., 2018**).

The tectonic landscape of Java is primarily shaped by subduction at the Java Trench, which has resulted in the formation of extensive magmatic belts, including Tertiary magmatic zones (**Soeria-Atmadja et al., 1994; Whitford et al., 1979**). The volcanic activity on the island is a direct result of this subduction process, and the Cenozoic volcanic arc history of East Java provides insight into the region's eruptive evolution (**Smyth et al., 2008**). Additionally, mountain ranges such as the Kendeng, Karangsambung, and Baribis Mountains contribute to Java's frequent tectonic activity (**Whitford et al., 1979**).

Recent studies underscore Java's significant earthquake potential, particularly in densely populated cities, such as Surabaya and Yogyakarta (**Pasari et al., 2021**). This seismic hazard is further intensified by seismic gaps south of the island, which pose a risk of megathrust earthquakes and tsunamis (**Widiyantoro et al., 2020**).

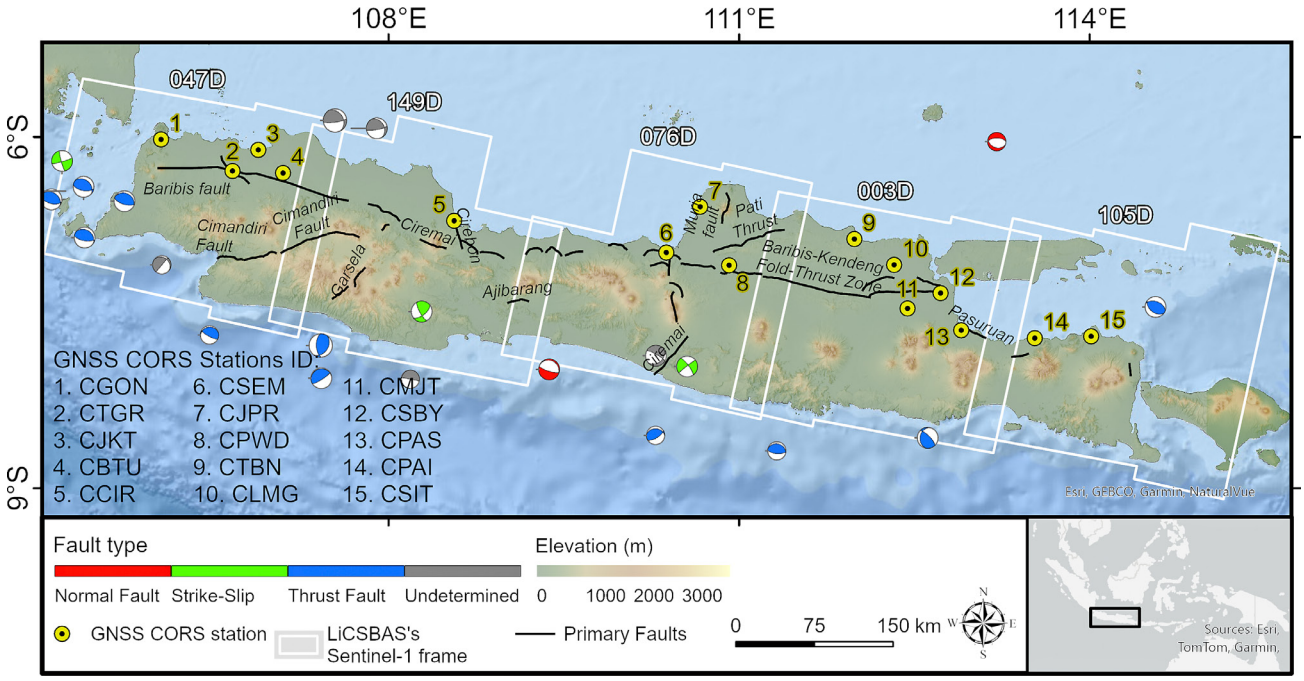

Figure 1. Java Island situation over complex geological and tectonic settings. The map includes significant earthquake epicenters and focal mechanisms (colored beach balls), primary crustal faults (black lines), GNSS continues monitoring (GNSS CORS) stations (yellow circles), and Sentinel-1 frames (white rectangles) used in this study. Primary fault data is sourced from the Indonesian National Earthquake Study Center (PuSGEN) v1.1 and the updated Baribis Fault from **Widiyantoro et al. (2020)**. GNSS station data is provided by the Indonesian Geospatial Agency (BIG) (2024). Sentinel-1 frame processing was conducted using LiCSAR, with further details available at the COMET LiCSAR portal (https://comet.nerc.ac.uk/comet-lics-portal/).

Although subsidence along Java's northern coast has been primarily attributed to human activities, preliminary studies indicate minimal tectonic influence (**Andreas et al., 2019**). However, the North-East to South-West (NE-SW) active faults in southern Java, combined with recent seismic activity, highlight the need for continued monitoring and assessment (**Arisbaya et al., 2021**). These findings underscore the complex and multifaceted nature of earthquake hazards on Java Island, with potential implications for its stability and safety (see **Figure 1**).

3. Material and Methods

3.1. Datasets

This study utilized five datasets from the descending tracks of Sentinel-1 SAR acquisition, which operate in the C-band with a wavelength of 5.547 cm and a right-looking direction (see **Figure 1**). The frames covering the entire Java Island, ranging from 047D to 105D, were selected for processing (see **Table 1**). The dataset spans from January 2017 to December 2022.

Data selection was consistent reasoning prior to 2017 since early Sentinel-1 acquisitions had greater than 12-day gaps due to its initial mission phase and Sentinel-1B's absence. Additionally, for scene 047D in 2023, only eight images were available, resulting in low coherence.

All selected datasets are interferograms provided by LiCSAR that were acquired in the Interferometric Wide (IW) mode, providing an appropriate width and spatial resolution for interferometry applications. IW data has a swath width of 250 km, 2.3 m pixel spacing in slant range and 14.1 m azimuth, and single-look resolution of 5 m in ground range and 20 m in azimuth. SRTM DEM with 30m resolution was used as the digital elevation model for processing.

Table 1. The basic specifications of the employed Sentinel-1 datasets in descending pass

Frame ID	Number of used acquisitions
047D_09652_111009	60
149D_09700_081210	65
076D_09725_121107	96
003D_09757_111111	58
105D_09782_131111	56

Several continuous GNSS monitoring (GNSS CORS) stations were employed, particularly across the north coast of the study area. The Indonesian Geospatial Information Agency (BIG) provided the CORS dataset that **Susilo et al. (2023)** processed using MIT/Global Kalman filtering (GAMIT/GLOBK) software. The data processing employs GAMIT software to apply double-differencing methods for processing GPS observations and estimating daily sta-

tion positions, atmospheric parameters, and other geophysical effects, with adjustments to align with IGS final orbits and corrections for ionospheric and tidal effects. In the second phase, GLOBK software integrates these daily solutions with global GPS solutions, aligning them to the ITRF2014 frame using Helmert transformation parameters, generating highly precise daily time series coordinates and ensuring integration with global positioning standards. This methodological approach enhances the accuracy of GNSS station positioning and seamlessly integrates with the IGB14 realization of ITRF2014.

3.2. *Methodology*

This study employed a systematic four-step methodology to generate and validate vertical displacement data from Sentinel-1 interferogram. The process began with downloading interferogram data from the LiCSAR database, which were processed using the SBAS approach for descending passes. Subsequently, Line-of-Sight (LOS) displacements were converted into vertical displacements. The displacement data were then classified into distinct categories to create a detailed deformation map. Finally, an accuracy assessment was conducted using GNSS measurements.

3.2.1. LiCSBAS

The Small Baseline Subset (SBAS) algorithm, a key technique in the Interferometric Synthetic Aperture Radar (InSAR) field, is designed to detect and analyze surface deformation over time. **Berardino et al. (2002)** and **Lanari et al. (2007)** provided overviews of the algorithm, with the latter presenting a quantitative performance analysis. **Hong et al. (2008)** introduced a related technique, the Small Temporal Baseline Subset (STBAS), for monitoring wetland water level changes. More recently, **Liu et al. (2020)** proposed a constrained SBAS method to address the rank deficiency problem that arises when interferograms are separated into multiple subsets. These studies collectively demonstrate the versatility and ongoing development of the SBAS algorithm for InSAR applications.

Morishita et al. (2020) developed LiCSBAS, an open-source InSAR time series analysis package that integrates with the LiCSAR automated Sentinel-1 InSAR processor. This tool has been shown to accurately detect and quantify surface displacements, making it a valuable asset in geodetic monitoring for hazard assessment. Unlike other InSAR processing tools, LiCSBAS does not require high-end computing power because the user does not need to process the interferogram, which is preprocessed and provided by the LiCSAR system. The application of LiCSBAS for surface deformation identification and analysis has proven particularly useful in a variety of geodetic monitoring scenarios, such as landslide monitoring, infrastructure stability assessment, and volcanic deformation analysis.

Interferograms were collected using the LiCSAR system throughout the study period. These interferograms were then unwrapped using the SNAPHU algorithm, which resolves the 2π ambiguities to retrieve absolute phase changes corresponding to land deformation. Following phase unwrapping, atmospheric corrections were applied using the Generic Atmospheric Correction Online Service (GACOS) weather model to mitigate atmospheric artifacts in the interferometric phases.

LiCSBAS also performed phase triangulation, linking unwrapped phases from multiple interferograms to generate a ground deformation time-series. The final deformation maps produced by LiCSBAS have a spatial resolution (~100 meters) lower than that of the original SAR images due to the multilook process employed by LiCSAR. The temporal resolution, however, is determined by the SAR acquisition frequency, which for Sentinel-1 is typically every 6–12 days. The software outputs included line-of-sight (LOS) displacement time series and velocity maps that depicted the deformation rate over the analyzed period.

LiCSBAS resulting displacement in LOS time-series and velocity map over the analyzed period and consisting of the incidence angle (θ) and satellite heading (α) for geometrical interpretation. LOS observations do not directly represent absolute ground motion but rather measure displacement towards or away from the satellite sensor. Therefore, as indicated by **Equation 1**, the standard approach computes the vertical displacement by assuming that horizontal motions are minimal (**Suhadha and Harintaka, 2024**).

$$\text{Vertical displacement} = \text{LOS} / \text{COS}(\theta) \quad (1)$$

The vertical displacement component was calculated by assuming predominantly vertical deformation, accounting for the satellite observation geometry. This is especially important in locations with mostly vertical ground movement since it allows for a more intuitive sense of magnitude and direction.

3.2.2. Deformation classification

Once the vertical displacement was calculated using the 2D approach, the data were classified into distinct

Table 2. Classification of deformation rates

Class	Deformation rate (cm)
Very High Subsidence	Less than -15
High Subsidence	-15 to -10
Moderate Subsidence	-10 to -5
Low Subsidence	-5 to -3
Stable	-3 to 3
Low Uplift	3 to 5
Moderate Uplift	5 to 10
High Uplift	10 to 15
Very High Uplift	More than 15

classes of deformation, measured in centimeters, to generate a heatmap that visually represents the variation in land deformation across the study area. These classes are defined as follows in **Table 2**.

This classification allowed to characterize and chart the extent of land deformation, from significant subsidence to tremendous uplift, for different areas. The deformation hotspot created a distinct and understandable portrayal of its landscape by correlating the vertical displacement values into these categories.

Upon classification and visualization, we focused on identifying areas of high levels of deformation, from highly deformed to low-magnitude zones. Under this analysis, the areas with the most significant effect of land deformation were determined, thereby making a more concerted study of the underlying causes and potential impacts possible.

The final step is to extract the zone(s) of the maximum deformation rates to perform a more concentrated time-series analysis of the deformation. It refers to removing the deformation data for a specified period to observe how the rate of deformation changes with time. By the time-series deformation, the temporal behavior of land motion could identify the trends and infer the causative mechanisms of the occurring deformation pattern.

3.2.3. Accuracy assessment

The Indonesian Geospatial Information Agency (BIG) GNSS CORS network data were employed to assure the reliability and accuracy of the displacement measurements obtained from InSAR. CORS stations, mainly located along Java Island's northern shore, have been provided with high-precision GPS receivers that provide continuous positional data for validation.

GNSS observations, prepared by **Susilo et al. (2023)**, were processed using RINEX GNSS files and filtered using the MIT/Global Kalman filtering software package to generate time-series station positions. Eleven CORS sites were selected, from which vertical displacement data during the observation time of InSAR were extracted. Displacement values derived from GNSS were spatially related to the nearest InSAR pixel so that the two data sets could be directly compared.

The Root Mean Square Error (RMSE) and Mean Relative Error (MRE) between the two data sets were calculated to assess the agreement between InSAR and GNSS measurements. By incorporating RMSE and MRE, vertical displacement accuracy from InSAR is evaluated based on absolute error magnitude and proportional impact compared to GNSS reference data. The dual-metric ap-

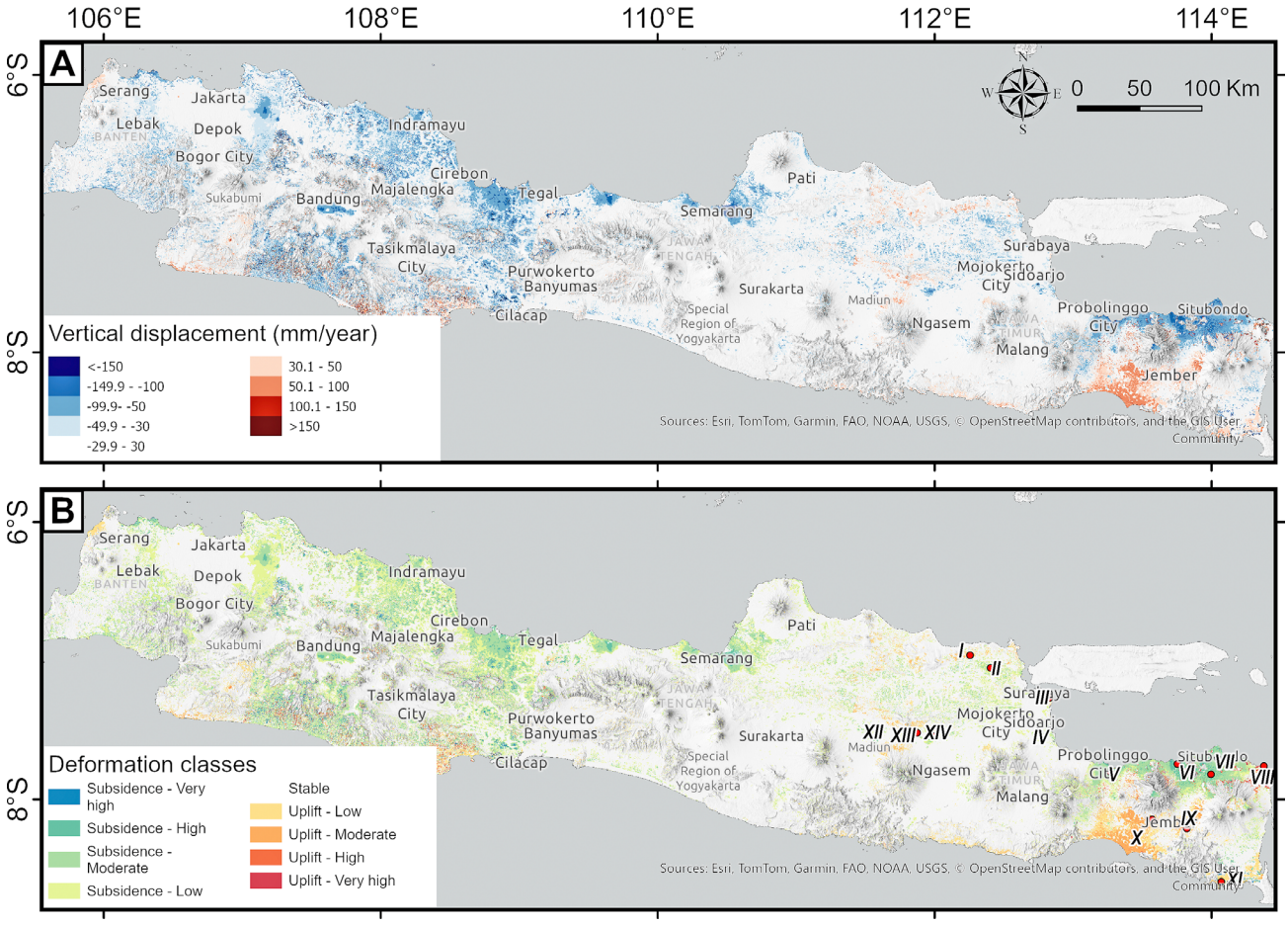

Figure 2. InSAR-derived displacement on a wide scale of Java Island is detailed for (A) vertical displacement and (B) deformation classification.

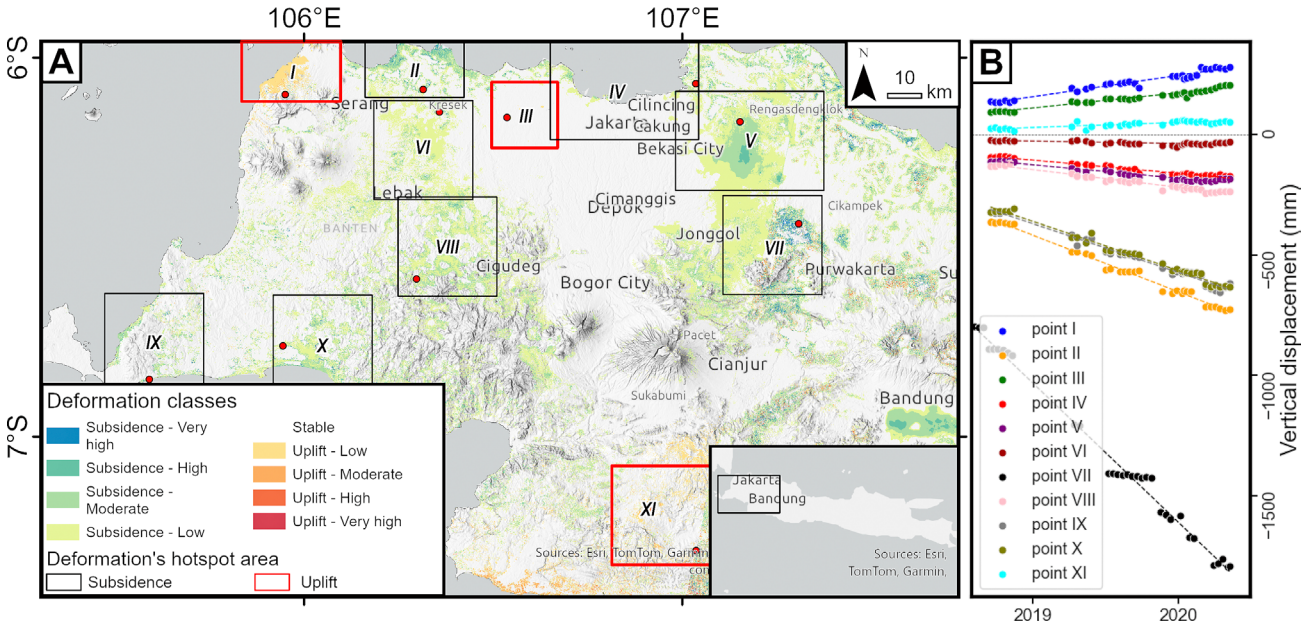

Figure 3. Land deformation analysis highlighting deformation hotspots in the first subset area, including Banten Province, Greater Jakarta, and the western part of West Java. (A) Deformation classification map for the first subset area, covering Banten Province, Greater Jakarta, and the western part of West Java Province. The map categorizes deformation into classes ranging from very high subsidence to very high uplift and identifies key hotspot areas. (B) Time-series plots illustrate the temporal evolution of vertical displacement at these hotspot points.

proach gives a complete evaluation, considering potential limitations and defining the reliability of the results.

4. Results

4.1. Overview

Sentinel-1 has revolutionized deformation monitoring, providing consistent observations due to its tightly controlled orbit and small perpendicular baselines, which help maintain high coherence across the study area. The vertical displacement patterns observed in **Figure 2** align with previous research, particularly in major cities experiencing linear subsidence from 2017 to 2022. For instance, Greater Jakarta recorded a maximum subsidence rate of -205 mm/year, with hotspot locations identified in Bekasi – an area previously underrepresented in similar studies.

Additionally, vertical deformation hotspot areas were detected using a classification based on geodynamic rate thresholds, categorizing deformation from low to very high for both subsidence and uplift. Several major cities on Java Island exhibit very high land subsidence velocities, including Bandung (-160 mm/year), Pekalongan (-152 mm/year), Probolinggo (-194 mm/year), Cirebon (-228 mm/year), and Semarang (-207 mm/year). Conversely, uplift was not limited to large urban areas but also affected surrounding regions. For example, western Jakarta (Tangerang) and Cilegon experienced moderate uplift, while Jember and Pangandaran recorded very high uplift rates of 589 mm/year and 167 mm/year, respectively.

The LiCSBAS processing framework, which implements a distributed scatterer InSAR approach, is susceptible to systematic bias due to decorrelation in densely vegetated and rapidly changing land cover areas. To mitigate this, a coherence threshold of 0.2 was applied to ensure spatial consistency while maintaining SAR phase reliability.

4.2. Deformation hotspot area

The study area was divided into four main subsets based on geological conditions, geohazard susceptibility, Sentinel-1 track coverage, and administrative boundaries to enhance the reliability of deformation monitoring. The associated Sentinel-1 LiCSAR tracks for each subset are as follows:

1. First Subset: Encompassing Banten Province, Greater Jakarta, and the western part of West Java Province, this area lies on the 047D Sentinel-1 track,
2. Second Subset: Covering the entirety of West Java Province, associated with track 149D,
3. Third Subset: Including Central Java Province on track 076D, this area features at least seven deformation hotspots,
4. Fourth Subset: Pertaining to East Java Province, this geologically complex area includes up to thirteen deformation hotspots across tracks 003D and 105D.

Each subset underwent a hotspot analysis, identifying key locations for further time-series vertical displacement monitoring.

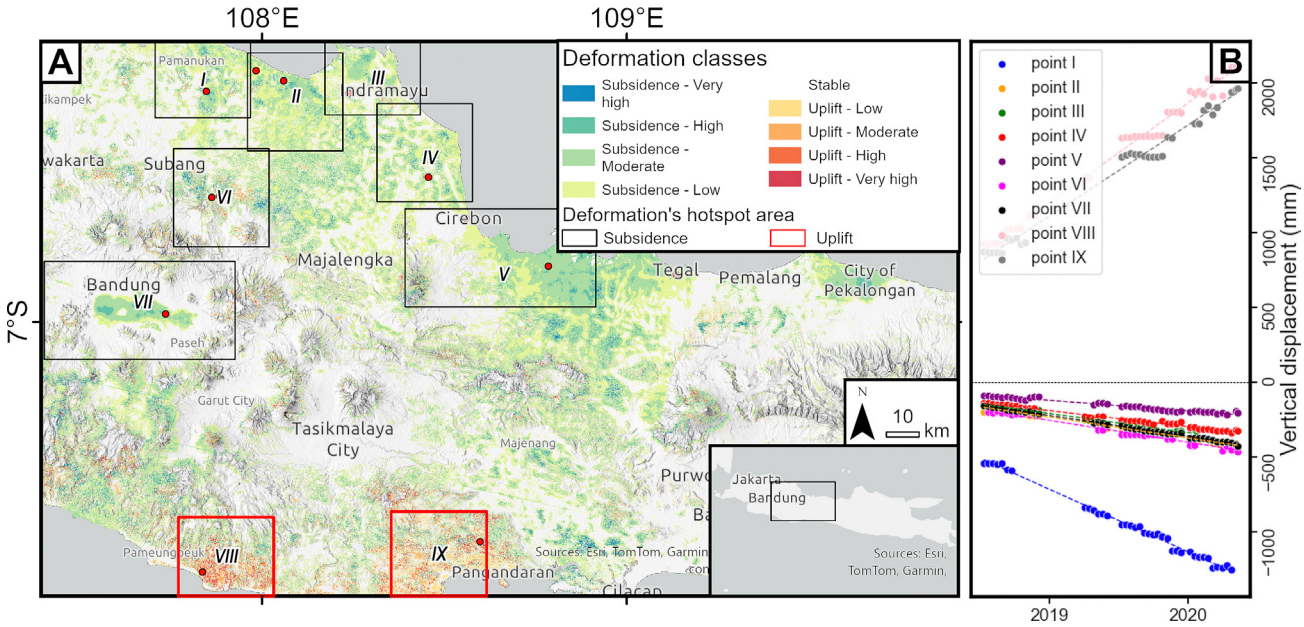

Figure 4. Land deformation analysis highlighting deformation hotspots in the second subset area, incorporating West Java Province. (A) Deformation classification map for the second subset area, encompassing West Java Province. Deformation is categorized from very high subsidence to very high uplift, with key hotspots highlighted. (B) Time-series plots provide the temporal trends of vertical displacement for the significant points.

The first subset, as illustrated in **Figure 3**, reveals a complex vertical displacement pattern between 2017 and 2021. Nine subsidence hotspots and three uplift locations were identified. The most severe subsidence occurred at Point VII (Ciampel, Karawang), reaching -1800 mm, followed by Point IV (Muara Gembong, Bekasi) and Point V (Cikarang), with rates of -200 mm and -180 mm, respectively. Moderate subsidence, up to -700 mm, was observed at Points II, IX, and X in Serang and along the southern coasts of Pandeglang and Lebak. In contrast, uplift movements were recorded at Point I (Cilegon), Point III (Pasarkemis, Tangerang), and Point XI (Sagaranten, Cianjur), each reaching +300 mm.

In the second subset area, presented in **Figure 4**, a total of nine deformation hotspots were detected, comprising seven subsidence and two uplift zones. Subsidence hotspots were scattered across Indramayu, Cirebon, Subang, and Bandung. Although Bandung has been the focus of recent subsidence research, it did not exhibit the most pronounced displacement in this study. Instead, the most severe ground sinking occurred at point I in Compreng, Subang, where subsidence reached 150 cm. This location, developed in the Cipunagara and Muara Curug rivers deltas, is prone to land sinking and flood inundation (**Solihuddin et al., 2021b, 2021a**). Conversely, the highest uplift was recorded at point VIII in Cibalong, Garut, with a displacement of 300 cm, followed by point IX in Pangandaran, which experienced an increase of 250 cm.

The third subset, covering Central Java Province, identified seven subsidence hotspots between 2017 and 2022, as shown in **Figure 5**. The most severe ground sinking occurred in Cilacap (point VI), with a displacement of -1200 mm in 2021, and in Semarang (point IV), where subsidence reached up to -1200 mm in 2022. While Semarang is a well-documented case of land subsidence (**Abidin et al., 2013a; Hakim et al., 2023**), this study revealed that Cilacap experienced even higher subsidence during the same period. The results indicate that Cilacap surpassed Semarang in subsidence magnitude, making it the most affected location in this subset. Additionally, point VII in Kulonprogo, Yogyakarta, which has been underrepresented in recent studies, recorded a maximum subsidence of 780 mm by the end of 2022. This level of displacement is comparable to Pekalongan's subsidence peak and is likely influenced by increasing land loads, reduced water infiltration, and aquifer depletion (**Hamdalah and Wibowo, 2020**).

Figure 6 presents the results for the last subset area, which includes East Java Province. This subset exhibits fourteen deformation hotspots, with five indicating uplift and nine showing subsidence. The most prominent uplift was detected in the southern and eastern coastal areas of Banyuputih, Situbondo, and Jember, where the terrain rose by up to 800 mm at points VIII, IX, and X. These locations are situated in an ancient volcanic field, where uplift may be influenced by ongoing mineralization and hydrothermal alterations (**Widiatmoko et al., 2021**). Uplift was also observed in Banyuwangi and Lamongan, where the terrain rose by 500 mm. While Banyuwangi shares geological characteristics with Jember, Lamongan is part of the Rembang Zone, a region known for wrench tectonism and basement-involved deformation, both of which may contribute to ground uplift (**Satyana et al., 2004**).

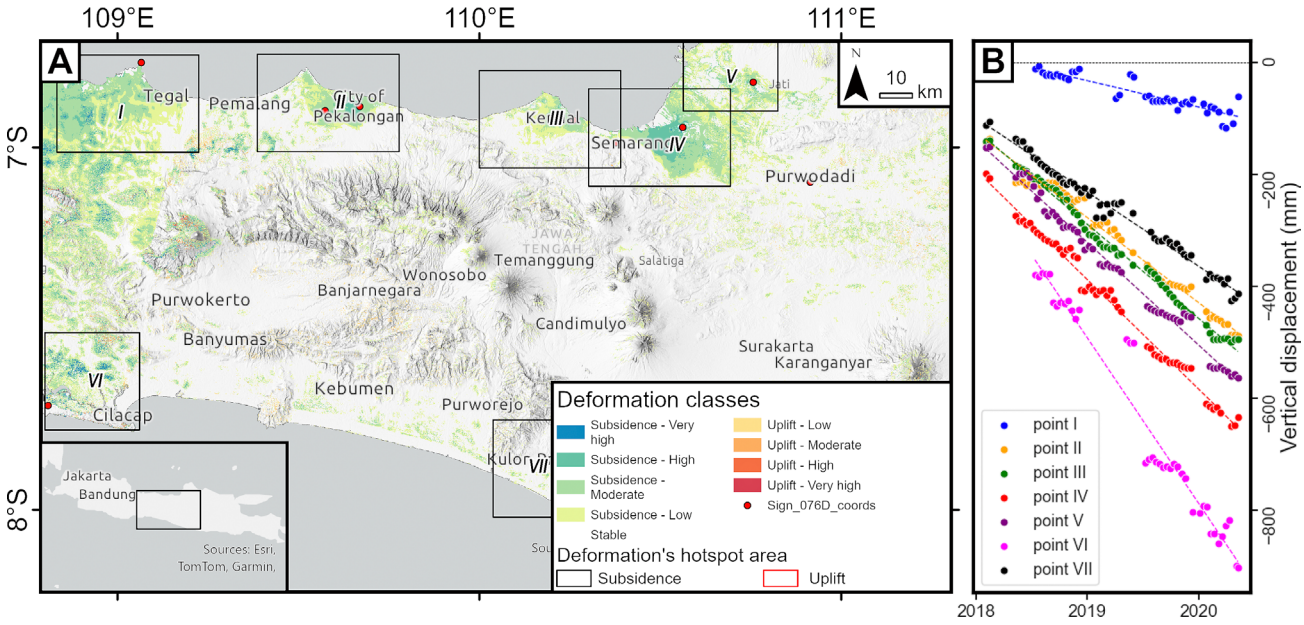

Figure 5. Land deformation analysis highlighting deformation hotspots in the third subset area, including Central Java Province. (A) Deformation classification map for the fourth subset area, spanning East Java Province. Deformation is classified from substantial subsidence to notable uplift, highlighting key deformation hotspots. (B) Time-series plots show the progression of vertical displacement over time for the significant points.

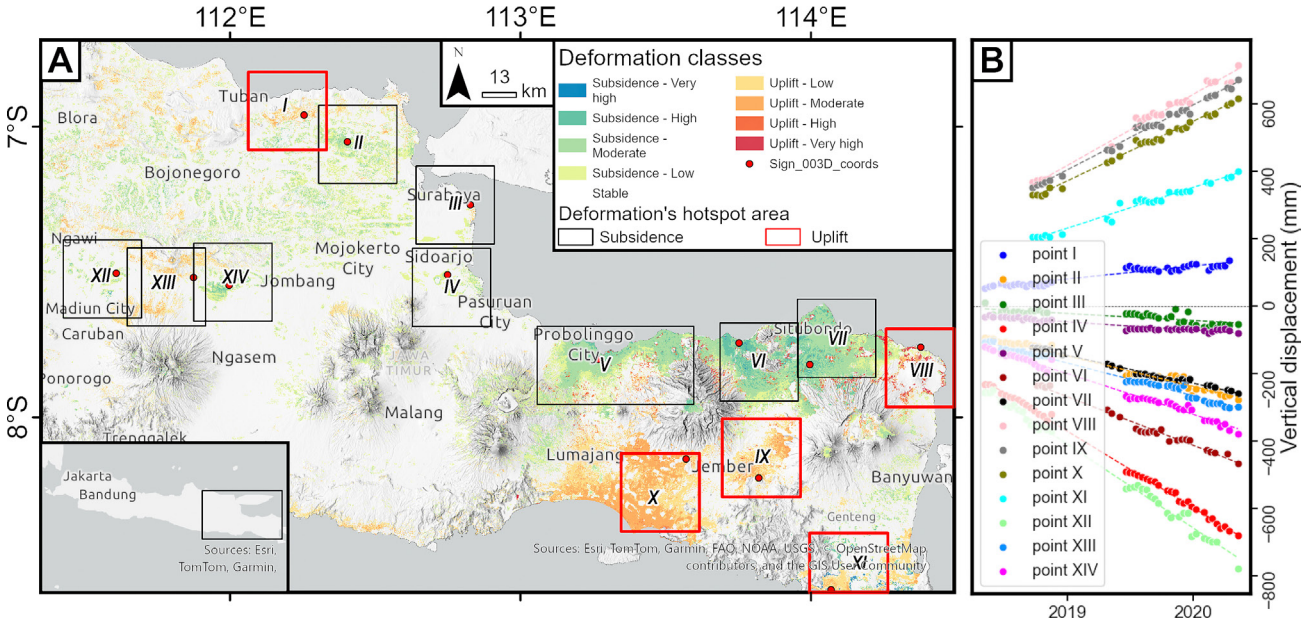

Figure 6. Land deformation analysis highlighting deformation hotspots in the fourth subset area, covering East Java Province. (A) Deformation classification map for the fourth subset area, spanning East Java Province. Deformation is classified from substantial subsidence to notable uplift, highlighting key deformation hotspots. (B) Time-series plots show the progression of vertical displacement over time for the significant points.

Conversely, substantial subsidence was recorded at points XII and XIII in Madiun and its surrounding cities, with maximum ground sinking reaching -1200 mm. Pilangkenceng subdistrict in Madiun, Rejoso in Madiun, and Gondang in Nganjuk experienced annual subsidence rates of -207.4 mm, -104.4 mm, and -200.2 mm, respectively. Although little prior research has focused on subsidence in these areas, historical flood events, particularly the catastrophic floods of 2019, suggest that ongoing land sinking has exacerbated flooding risks (**Susilo et al., 2021**).

Additional significant subsidence events were identified in the Surabaya metropolitan area and Porong, Sidoarjo. In Surabaya, rapid urbanization and high-water demand have resulted in extensive groundwater extraction, leading to a subsidence rate of -140 mm by the

Table 3. Comparison of InSAR and GNSS displacement measurements, including standard deviation, RMSE, and MRE at various GNSS stations.

Station ID	STD InSAR	STD GNSS	InSAR vs GNSS RMSE	InSAR vs GNSS MRE
CBTU	0.71	0.90	1.90	5.86
CCIR	0.70	1.03	2.14	3.44
CGON	1.33	0.96	2.24	2.66
CJKT	0.84	1.01	1.57	1.21
CJPR	0.88	1.20	2.15	3.13
CLMG	0.44	1.26	2.04	1.93
CMJT	0.35	0.88	0.95	1.65
CPAI	1.45	1.00	2.60	11.22
CPAS	0.56	0.67	0.87	3.23
CPWD	0.70	1.12	1.28	3.03
CSBY	0.54	1.03	1.05	5.51
CSEM	0.66	1.01	1.34	5.26
CSIT	2.77	0.93	2.58	14.81
CTBN	0.65	1.04	1.51	7.63
CTGR	0.80	1.06	1.76	1.86

Note:
Station ID: Identifier for GNSS stations.
STD InSAR: Standard deviation of InSAR-derived displacement (cm).
STD GNSS: Standard deviation of GNSS-derived displacement (cm).
RMSE (Root Mean Square Error): Measure of the differences between InSAR and GNSS displacement values (cm).
MRE (Mean Relative Error): Mean relative error between InSAR and GNSS displacements (%).

end of 2021 (**Aditiya et al., 2017**). Meanwhile, in Porong, Sidoarjo, where land sinking has been continuously observed since the 2006 Lusi mud eruption, the maximum recorded subsidence reached -1100 mm, particularly in the southern and western sectors. Further analysis of subsidence in the Probolinggo-to-Situbondo region (points V–VII) revealed high displacement levels, with maximum recorded subsidence of -160 mm, -600 mm, and -300 mm, respectively, in early 2021.

4.3. Comparison with GNSS Measurements

Vertical displacement data derived from InSAR were compared with GNSS measurements recorded by the CORS network of the Geospatial Information Agency of Indonesia (BIG) between 2017 and 2022. The comparison was based on RMSE and MRE values across 15 monitoring stations, as summarized in **Table 2**.

Most stations exhibited RMSE values below 2.5 cm, indicating a reasonable level of agreement between the two datasets, especially considering that the subsidence rate is near or exceeds 10 cm. Notably, stations CMJT, CPAS, and CSBY exhibited RMSE values of 0.95 cm, 0.87 cm, and 1.05 cm, respectively, with corresponding MRE values of 1.65%, 3.23%, and 5.51%, confirming the high precision of InSAR-derived measurements.

However, stations CPAI and CSIT displayed higher RMSE values of 2.6 cm and 2.58 cm, along with elevated MRE values of 11.22% and 14.81%, respectively. These discrepancies are associated with greater variability in InSAR data, as indicated by higher standard deviations (e.g. CSIT with an STD of 2.77 cm). **Figure 7** presents scatter plots illustrating these results, showing a strong correlation between InSAR-derived displacements and GNSS measurements, with most stations clustering near the 1:1 trend line.

Overall, the findings confirm that InSAR provides reliable vertical displacement measurements, with strong agreement observed at most monitoring stations. The low MRE values recorded at stations such as CMJT (1.65%) and CLMG (1.93%) further validate the accuracy of InSAR-derived displacements across the study area.

5. Discussion

5.1. Deformation Hotspots and Trends

Java Island subsidence research has been focused on capital cities, including Jakarta, Semarang, Bandung, Pekalongan, and Surabaya (**Chaussard et al., 2013; Khakim et al., 2013; Sarah et al., 2023; Sidiq et al., 2021**). Whereas Jakarta has frequently been quoted as one of the world's fastest-sinking cities, with up to 17 cm/year subsidence rates (**Takagi et al., 2023**), here it is implied that some cities have even higher subsidence rates. Three yet-to-be-published cities – Karawang, Cilacap, and Madiun – exhibit extremely high land sub-

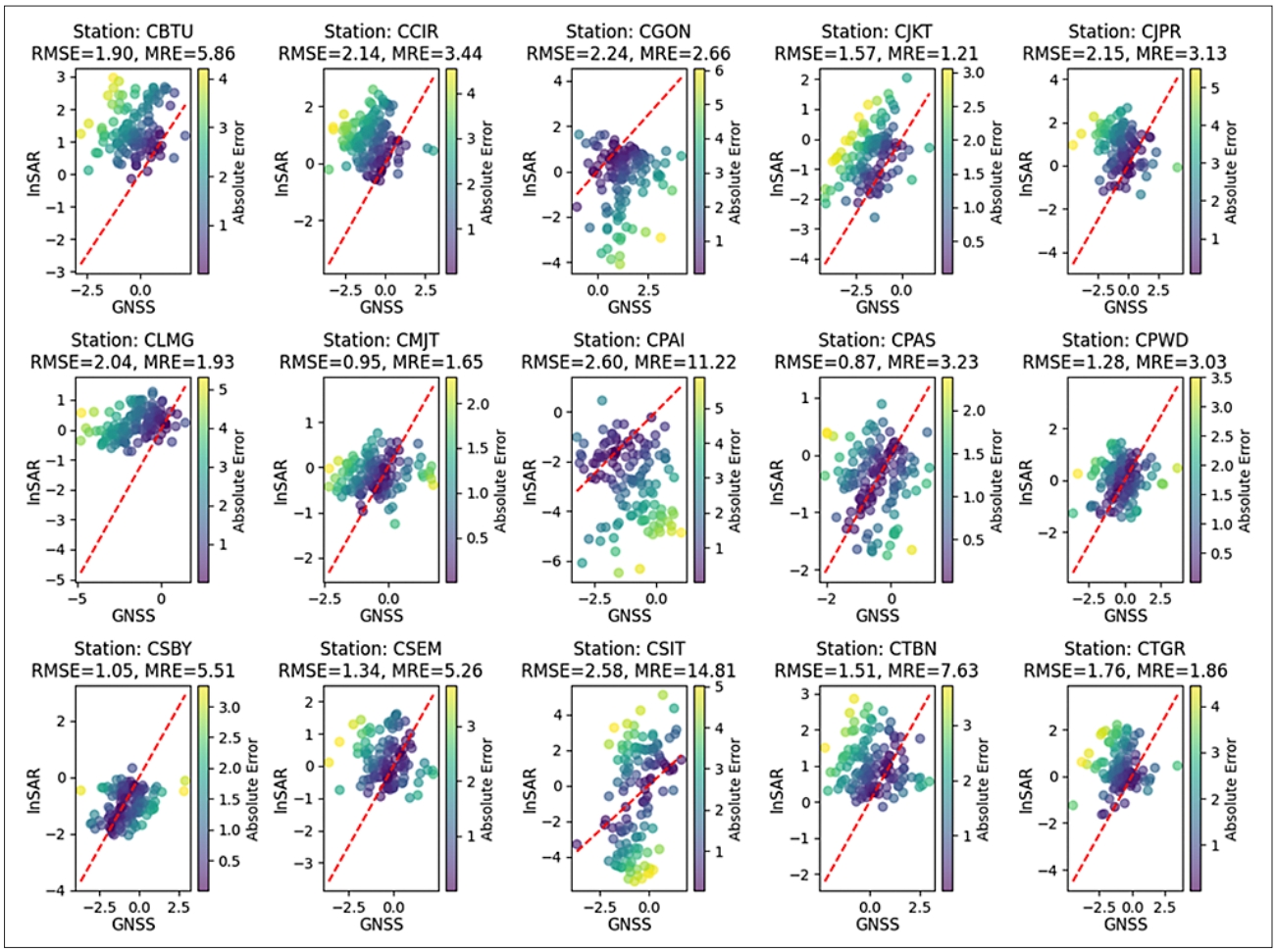

Figure 7. Scatter plots comparing GNSS (observed displacement) and InSAR (predicted displacement) at various GNSS-CORS stations, with RMSE (Root Mean Square Error) and MRE (Mean Relative Error) annotated. Each plot highlights the relationship and absolute errors for data up to 2022, with a red dashed line representing the ideal 1:1 correspondence.

sidence above 150 mm/year, where the monitoring necessity also needs to be extended beyond provincial capital cities.

Validation using GNSS data (see **Figure 7**) confirms the reliability of InSAR-derived displacement measurements, with most stations demonstrating low RMSE values below 2 cm. Given that this study focuses on large-scale deformation monitoring, the observed RMSE values are well within an acceptable range relative to the magnitude of detected subsidence. However, localized discrepancies emerge at certain stations, notably CPAI and CSIT, where RMSE values of 2.6 cm and 2.58 cm and elevated MRE values of 11.22% and 14.81% indicate significant local variations in ground movement. These differences are most likely due to increased atmospheric perturbation, local geological inhomogeneity, or phase unwrapping challenges in regions of intricate deformation patterns. Despite these differences, the strong correlation between InSAR and GNSS measurements supports the reliability of Sentinel-1 data for regional deformation monitoring.

Figure 8 presents a comparative summary of the major land subsidence locations, while **Table 3** details site characteristics, including maximum rates of subsidence and ground environment. Previous subsidence studies in Java have mainly centered on northern coastal cities, such as Jakarta, Semarang, and Pekalongan, due to their high urbanization and vulnerability to coastal subsidence. However, the research reveals that severe land subsidence also occurs in inland, peri-urban, and southern coastal regions. These areas, which are witnessing rapid urban expansion, industrialization, and increasing groundwater abstraction for domestic, industrial, and agricultural uses, exhibit extensive ground deformation.

A progressive and almost linear pattern of land subsidence at different locations, as indicated in **Figure 8**, indicates a uniform ground-acceleration sinking. The most extreme cases occur in Karawang, which experienced a dramatic subsidence of -1795 mm in 2022, followed by Cilacap (-902 mm) and Madiun (-742 mm) (see **Table 4**). These regions display a consistent trend of continuous subsidence over time. Additionally, subsidence in peri-urban and industrial expansion areas such as Bekasi-1, Bekasi-2, and Serang remains persistent, albeit at a moderate rate. These findings emphasize the necessity of expanding subsidence monitoring beyond

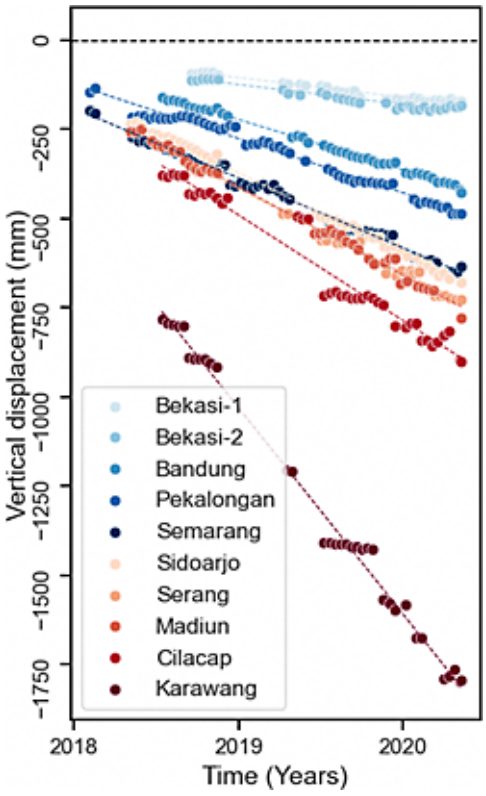

Figure 8. Time-series of vertical displacement on the subsidence peak areas (sequential red dots) comparison with the previous known subside locations (sequential blue dots)

major metropolitan areas, ensuring a more comprehensive understanding of land deformation dynamics across Java Island.

5.2. *Triggering factors in the top five highest land subsidence*

Land subsidence in Indonesia is predominantly driven by human activities, particularly groundwater and other fluid extraction. However, natural factors such as natural consolidation, volcanic activity, and tectonic movements also contribute to the ground sinking in certain regions (**González et al., 2015; Khakim et al., 2023; Suhadha and Harintaka, 2024; Zaenudin et al., 2018**). In many cases, the interaction between natural and anthropogenic forces accelerates both the rate and severity of ground displacement.

Previous studies, including **Khakim et al. (2023)**, **Sidiq et al. (2021)**, and **Solihuddin et al. (2021a)**, primarily focused on major cities, leaving several smaller but significant subsidence-prone areas undetermined due to minimal recorded displacement or data limitations. Previous analysis, based on ALOS PALSAR (L-band SAR), provided better penetration in vegetated areas. However, it suffered from low temporal resolution, susceptibility to atmospheric noise, and potential DEM errors, which likely underestimated subsidence in some locations (**Chaussard et al., 2013; Fukushima, 2023; Morishita et al., 2023**). As a result, several non-urban or peri-urban regions with significant subsidence remained underrepresented.

5.2.1. Significant location 1: Karawang (with a maximum of -1795 mm)

Karawang has experienced the most severe subsidence on Java Island, with a peak of -1795.53 mm in mid-2020, aligning with the initial findings of **Julzarika (2024)**. The Telukjambe Timur region, through which the Citarum River flows, as well as the Bekasi-Purwakarta segment of West Java Back-arc Thrust (Baribis Fault) (**Susilo et al., 2022**), is predominantly composed of soft alluvial and Miocene sediments, making it highly susceptible to natural compaction. This vulnerability is exacerbated by external factors such as groundwater depletion and infrastructure development (see **Figure 9A**). Additionally, the proximity of the affected area to the Baribis Fault suggests a potential tectonic influence on subsidence patterns.

Karawang has undergone rapid urbanization and industrial expansion, as depicted in **Figure 10B**, where large-scale manufacturing and logistics developments have replaced previously vegetated areas. Moreover, groundwater extraction plays a dominant role in accelerating subsidence. As shown in **Figure 10C**, the most pronounced land displacement coincides with the peak decline in Land Water Equivalent (LWE) (2019-2020), indicating aquifer compaction due to excessive fluid withdrawal. The combined impact of geological vulnerability, industrialization, and groundwater depletion has made Karawang one of the most critical subsidence hotspots on Java Island.

Table 4. Top five locations of the highest land subsidence on the Island of Java

Subsidence occurrences					
No	**Figure/Point**	**Location**	**Subdistrict, City**	**Maximum subsidence (mm)**	**Nature of point**
1.	4/VII	-6.437, 107.307	Ciampel, Karawang	-1795.53	Local roads
2.	6/VI	-7.711, 108.807	South Cilacap, Cilacap	-902.234	Open area
3.	7/XII	-7.504, 111.607	Pilangkenceng, Madiun	-742.247	Road
4.	4/II	-6.083, 106.314	Carenang, Serang	-727.892	Pady field embankment
5.	7/IV	-7.509, 112.748	Porong, Sidoarjo	-680.114	Paddy field embankment

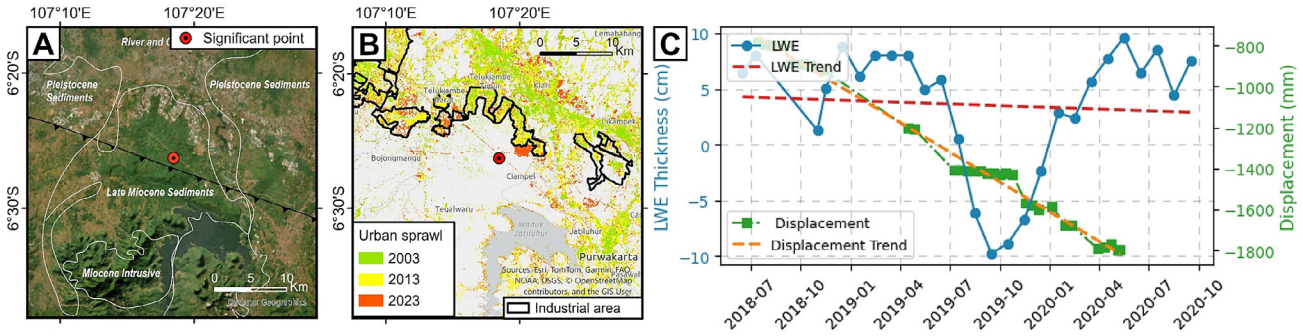

Figure 9. Triggering factors analysis of the significant location in Karawang. (A) The location of the significant subsidence point in Karawang is overlaid on satellite imagery that is overlayed with the geological setting. (B) Urban expansion from 2003 to 2023, highlighting industrial growth in the region. (C) Time-series of Land Water Equivalent (LWE) and vertical displacement.

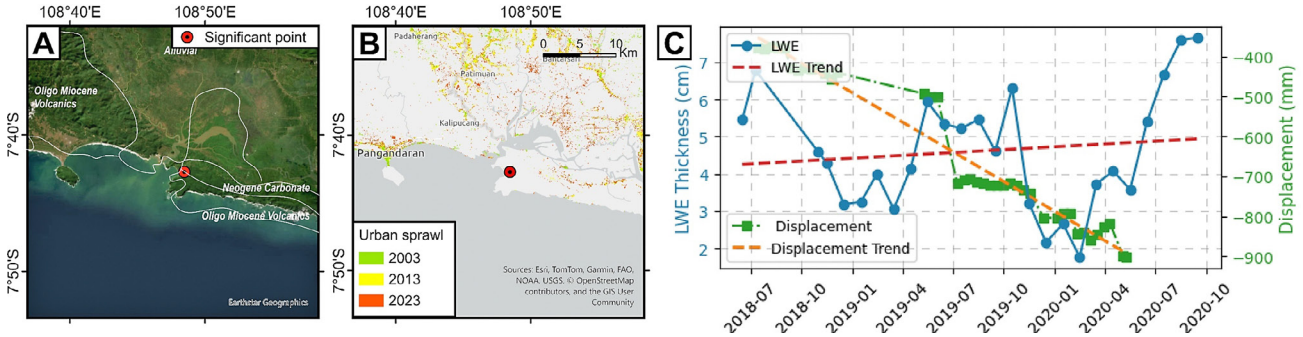

Figure 10. Triggering factors analysis of the significant point in Cilacap. (A) Significant subsidence point in Cilacap shown on satellite imagery overlayed with the geological setting. (B) Urban growth between 2003 and 2023, illustrating land-use changes in coastal and industrial areas. (C) LWE and displacement trends from 2018 to 2020.

5.2.2 Significant location 2: Cilacap (with a maximum of -902.234 mm)

Cilacap, particularly South Cilacap, experiences significant coastal subsidence, reaching -902 mm, primarily driven by natural sediment compaction and groundwater depletion. Geologically, as shown in **Figure 10A**, the area is dominated by volcanic deposits and carbonate formations. At the selected significant point, alluvial deposits raise as the dominant form, which is naturally susceptible to compaction due to the weight of overlying sediments and tectonic forces, especially in coastal and estuarine environments (**Karadenizli, 2011; Kralj, 2012; Pomar et al., 2015; Noufal and Shebl, 2019**).

Both fluvial and marine processes influence the coastal morphology of Cilacap. The interaction between river sediment inputs and marine redistribution affects the stability and development of coastal landforms (**Kurnio, 2007**). Additionally, **Figure 10C** shows a clear correlation between declining LWE and increased subsidence, confirming that groundwater decreasing is a key contributor to land sinking. Recent studies indicate that at least three districts in Cilacap have a moderate vulnerability to seawater intrusion and shallow interface depth owing to their heavy water demand for domestic and industrial purposes, making it more pronounced for land subsidence (**Edison et al., 2021; Nugrahaeni et al., 2021; Purnama, 2019**).

However, a contrasting finding from **Andreas et al. (2018)** reported no significant vertical land motion based on continuous GNSS station measurements in Cilacap. In contrast, the coastal-riverine setting of Nusa Kambangan appears more susceptible to compaction-driven subsidence, likely due to its soft alluvial deposits and fluctuating groundwater conditions. Furthermore, a geoelectric study by **Andi and Setiahadiwibowo (2020)** detected subsurface cavities, suggesting that the area is prone to sinkhole formation, potentially exacerbating localized land instability.

5.2.3 Significant location 3: Madiun (with a maximum of -742.247 mm)

Madiun occupies a basin on the eastern side of Java Island, Indonesia, where its alluvial deposit is inherently liable to subsidence. Subsidence also stems from overextraction of groundwater and land use change. Quaternary thick sediments greater than 250 meters form one of the causative factors because deep sediment deposits consisting of sand, silts, and clays of over 250 meters are highly prone to compaction under particular circumstances (**Kumazawa, 1994**).

The declining Land Water Equivalent (LWE) trend (see **Figure 11C**) closely correlates with increasing displacement, confirming that subsidence in Madiun is primarily driven by excessive groundwater extraction, par-

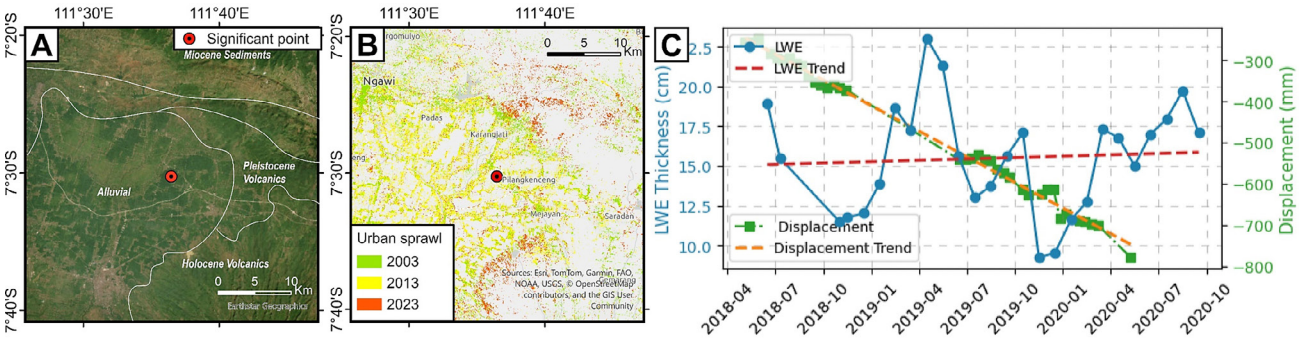

Figure 11. Triggering factors analysis of the significant location in Madiun. (A) The location of the major subsidence point in Madiun shown on satellite imagery overlayed with the geological setting. (B) Urbanization trends from 2003 to 2023 show the expansion of urban areas in the location. (C) Time-series of LWE and displacement from 2018 to 2020.

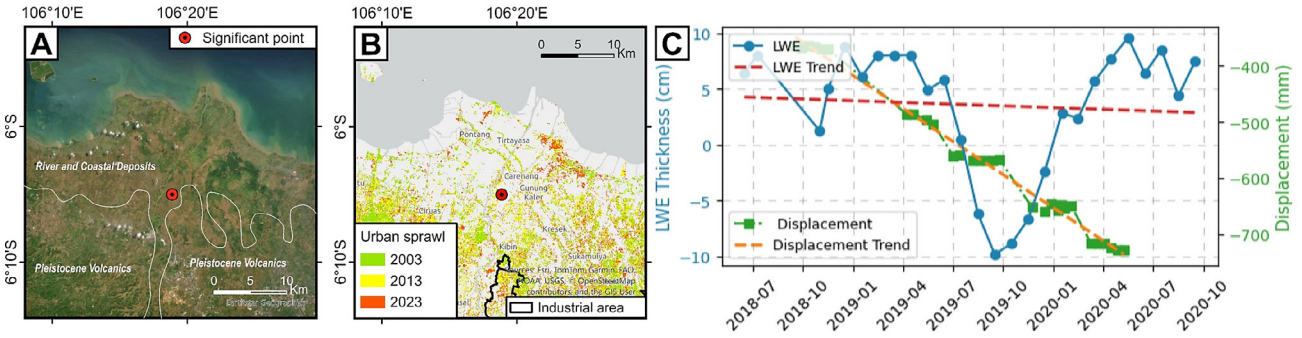

Figure 12. Triggering factors analysis of the significant location in Serang. (A) The location of the observed subsidence point in Serang shown on satellite imagery overlayed with the geological setting. (B) Urban and industrial expansion from 2003 to 2023, indicating increasing land-use changes. (C) LWE and displacement trends from 2018 to 2020.

ticularly for urban supply and irrigation purposes. Several studies support this finding, highlighting that most paddy fields in Madiun rely on groundwater pumping, resulting in high withdrawal rates from both shallow and deep wells (**Aqil et al., 2007; Nugraha et al., 2023**). Consequently, Madiun exhibits a high potential for land subsidence, as evidenced by this study.

An official report from Indonesia's Ministry of Energy and Mineral Resources indicated that Balerejo District in Madiun experienced up to 20 meters of subsidence between 2007 and 2019 (**Pribadi, 2019**). The findings of this study corroborate the government report, providing a detailed time-series perspective on subsidence progression. Moreover, Madiun's urban expansion into formerly agricultural areas increases surface load, further compacts soft sediments, and reduces groundwater recharge capacity, speeding up land subsidence. Policy responses to slow both the rate and impact of land subsidence in the region are urgently required to mitigate this issue.

5.2.4 Significant location 4: Serang (with a maximum of -727.892 mm)

The northern coastal plain of Java consists of unconsolidated Holocene alluvial deposits, making it highly susceptible to natural compaction and land subsidence (**Han et al., 2018; Sarah, 2022**). This geological vulnerability also extends to Banten Province, which remains underrepresented in subsidence studies compared to other provinces. The findings of this study indicate that Serang, largely composed of riverine and coastal sediment deposits, is particularly vulnerable to land subsidence. The combination of geologically fragile conditions, rapid industrial expansion, and excessive groundwater depletion has resulted in subsidence reaching -727 mm by the end of 2022 (see **Figure 12**).

Despite these alarming findings, land subsidence in Serang has long been underestimated in scientific research in relation to other vulnerable regions such as Jakarta and Semarang (**Asdak et al., 2018; Lubis et al., 2011; Takagi et al., 2016**). The lack of comprehensive studies and continuous monitoring activities hinders the application of effective mitigation measures. As Serang becomes increasingly a center for industry and residence, land-use planning and the sustainable management of water resources must be integrated into local policy to prevent further land subsidence. Increasing long-term geodetic observation and multi-sensor remote sensing studies is critical to addressing this neglected but pressing issue.

5.2.5 Significant location 5: Sidoarjo (with a maximum of -680.114 mm)

Sidoarjo's alluvial deposits and Pleistocene sediments make it naturally prone to subsidence, a condition fur-

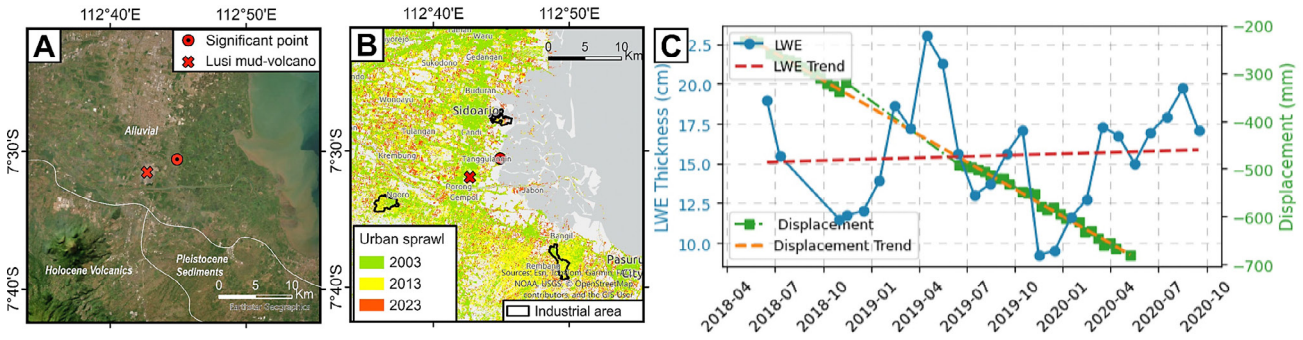

Figure 13. Triggering factors analysis of the significant location in Sidoarjo. (A) Major subsidence point in Sidoarjo, with proximity to the Lusi mud volcano. (B) Urban sprawl from 2003 to 2023, depicting rapid industrialization and land conversion. (C) Time-series of LWE and displacement, showing groundwater depletion as a key factor influencing subsidence, alongside the impact of the mud volcano.

ther exacerbated by the ongoing influence of the Lusi mud volcano, which continues to induce sediment deformation and underground fluid migration (**Fikri et al., 2021**). With a recorded land subsidence of -680 mm, this region is significantly impacted by a combination of geological instability, rapid industrial expansion, excessive groundwater extraction, and the persistent effects of the Lusi mud eruption. The influence of the Lusi mud volcano in this area has been extensively documented (**Fukushima et al., 2009; Hayati et al., 2022; Yulyta et al., 2016**), and this study confirms that vertical land displacement remains active today.

The strong correlation between declining LWE and increasing subsidence underscores the urgent need for groundwater regulation and sustainable land-use planning to mitigate further subsidence in this highly industrialized area (see **Figure 13**). Among the most affected regions, Sidoarjo has long been recognized for its severe subsidence, largely attributed to the Lusi mudflow disaster and extensive subsurface fluid extraction (**Hadianti and Dewanto, 2023**).

5.3. *Earth equilibrium in Java Island*

The Earth's surface acts as a dynamic system where volume and area variations are relatively steady, and a constant state of equilibrium is required within land deformation processes (**Turcotte and Schubert, 2014; Nelson and Cottle, 2017**). This is manifested in synchronous subsidence in some regions and uplift in others, both geologically and anthropogenically.

Along coastal regions such as Karawang, Tegal, Probolinggo, and Situbondo, coastal protection structures constructed to counter erosion frequently interfere with sediment balance, leading to sediment deficits in the nearby regions. The deficits increase subsidence rates through the alteration of patterns of sediment deposition and removal (**Solihuddin et al., 2021b**). This phenomenon expresses the overall principle of surface deformation, where a set of parameters – such as sediment supply and removal, groundwater utilization, and geology – conjointly determine vertical land motion.

Groundwater extraction plays a particularly significant role in land subsidence, as it reduces hydrostatic pressure within aquifers, increasing geostatic stress and leading to soil compaction (**Julzarika et al., 2023, 2018**). Terzaghi's law describes this relationship, emphasizing how changes in groundwater pressure directly impact soil deformation and land stability. Additionally, soil composition influences the subsidence rate, with coarser sands being more prone to rapid compaction, whereas finer-grained sediments exhibit greater resistance to deformation.

Therefore, the dynamic equilibrium of Earth's topography is maintained through the continuous interplay of uplift and subsidence forces, shaped by both natural processes and human activities. While local and regional topographic variations persist, these opposing forces contribute to long-term stability in the global land-to-water ratio over geological timescales.

5.4. *InSAR-derived Land subsidence Hotspots: Large-Scale Challenges and Opportunities*

This study has identified numerous previously unanticipated vertical land motion hotspots across Java Island, emphasizing the necessity for a new strategy for land subsidence management. These results could prompt researchers and government agencies to adopt new strategies for mapping, modeling, and mitigating underrepresented subsidence-prone areas. However, the limited number of GNSS stations used for validation introduces potential uncertainties in the results. This emphasizes the need for expanding continuous GNSS monitoring networks, which remains challenging due to financial and logistical constraints. Strengthening the geodetic monitoring infrastructure would enhance the reliability of deformation measurements and support the integration of InSAR and GNSS data for improved accuracy (**Abidin et al., 2013b; Fabris et al., 2022; Liu et al., 2019**).

Meanwhile, InSAR has further solidified its role as an essential tool for high-precision surface deformation monitoring, especially in tropical regions. Future re-

search should focus on denser InSAR observations, validated with GNSS, across other Indonesian Islands to uncover additional surface deformation hotspots, particularly in underrepresented regions. Moreover, upcoming SAR missions, such as NISAR (**Rosen et al., 2016**) and recently launched satellites like Sentinel-1C and ALOS-4 PALSAR-3 (**Motohka et al., 2019**), are expected to enhance vegetation penetration and temporal resolution, making them better suited for deformation monitoring in Indonesian landscapes.

6. Conclusions

Understanding Vertical Land Motion (VLM) is significant for geological hazard estimation, urban planning, and infrastructure resilience. Java Island is a geodynamically complex region with subsidence and uplift due to anthropogenically driven and natural processes. Although previous studies in Java Island were predominantly focused on significant cities such as Jakarta, Bandung, and Semarang, systematic large-scale observation in small, unrepresented regions was lacking.

This study uses a Small Baseline Subset (SBAS) InSAR to map VLM across Java Island completely, combining multi-temporal satellite data with GNSS validation. The hotspots of subsidence identified are notable, with Karawang (-1795 mm), Cilacap (-902 mm), and Madiun (-742 mm) suffering from increased ground subsidence compared to Jakarta coastal areas. Uplift trends in East Java are also due to tectonic and volcanic forces. The findings highlight the need for local monitoring to fully appreciate land deformation's main reasons and spatial gradients.

Besides confirming well-documented places of subsidence risk, the study identifies previously unreported zones such as Madiun, Cilacap, and Serang that now register elevated levels of subsidence. Policymakers and urban planners rely on the data, which prompts improved water resource management, land-use planning, and infrastructure realignment in areas prone to this phenomenon.

Despite the power of SBAS InSAR for large-scale monitoring, there are still some limitations, including potential biases from GNSS station density and atmospheric delays. Future research will likely focus on denser GNSS networks, higher resolution InSAR observations, and multi-sensor integrated solutions to improve displacement accuracy. Moreover, future SAR missions of NISAR, Sentinel-1C, and ALOS PALSAR-4 will have enhanced vegetation penetration and temporal resolution, further enhancing deformation monitoring performance.

Finally, this research reiterates the value of Earth Observation technologies for the study of long-term land deformation. This study provides high-precision deformation mapping and insight into Java's evolving geodynamics by integrating advanced InSAR time-series processing and ground-based validation. Enhancing routine and spatially dense monitoring campaigns will play a very important role in developing effective mitigation strategies against land subsidence and uplift hazards, facilitating sustainable development across Java Island.

Acknowledgement

Sentinel-1 data were provided by the European Space Agency (ESA), processed by LiCSAR, and further analyzed using LiCSBAS for time-series analysis. The GNSS data are provided by the Indonesian Geospatial Agency (BIG). All data processing was done using BRIN's High Performance Computer (HPC).

7. References

Abidin, H., Andreas, H., Gamal, M., Gumilar, I., Napitupulu, M., Fukuda, Y., Deguchi, T., Maruyama, Y., Riawan, E., (2010). Land subsidence characteristics of the Jakarta basin (Indonesia) and its relation with groundwater extraction and sea level rise 113–130. https://doi.org/10.1201/b10530-11

Abidin, H.Z., Andreas, H., Gumilar, I., Fukuda, Y., Pohan, Y.E., Deguchi, T., (2011). Land subsidence of Jakarta (Indonesia) and its relation with urban development. Natural Hazards 59, 1753–1771. https://doi.org/10.1007/s11069-011-9866-9

Abidin, H.Z., Andreas, H., Gumilar, I., Sidiq, T.P., Fukuda, Y., (2013a). Land subsidence in coastal city of Semarang (Indonesia): Characteristics, impacts and causes. Geomatics, Natural Hazards and Risk 4, 226–240. https://doi.org/10.1080/19475705.2012.692336

Abidin, H.Z., Andreas, H., Gumilar, I., Sidiq, T.P., Fukuda, Y., (2013b). On the Roles of Geospatial Information for Risk Assessment of Land Subsidence in Urban Areas of Indonesia, in: Zlatanova, S., Peters, R., Dilo, A., Scholten, H. (Eds.), Lecture Notes in Geoinformation and Cartography. Springer-Verlag, Berlin, Heidelberg, pp. 277–288. https://doi.org/10.1007/978-3-642-33218-0_19

Abidin, H.Z., Andreas, H., Gumilar, I., Wibowo, I.R.R., (2015). On correlation between urban development, land subsidence and flooding phenomena in Jakarta. IAHS-AISH Proceedings and Reports 370, 15–20. https://doi.org/10.5194/PIAHS-370-15-2015

Aditiya, A., Takeuchi, W., Aoki, Y., (2017). Land Subsidence Monitoring by InSAR Time Series Technique Derived from ALOS-2 PALSAR-2 over Surabaya City, Indonesia. IOP Conf Ser Earth Environ Sci 98. https://doi.org/10.1088/1755-1315/98/1/012010

Andi, Setiahadiwibowo, A.P., (2020). Identifikasi rongga menggunakan metode geolistrik konfigurasi dipole-dipole daerah Nusakambangan Cilacap Jawa Tengah. Kurvatek 5, 47–54. https://doi.org/10.33579/KRVTK.V5I2.2005

Andreas, H., Abidin, H.Z., Sarsito, D.A., Meilano, I., Susilo, (2018). Investigating the tectonic subsidence on Java Island using GNSS GPS campaign and continuous. AIP ConfProc 1987. https://doi.org/10.1063/1.5047376/909536

Andreas, H., Zainal Abidin, H., Anggreni Sarsito, D., Meilano, I., Susilo, S., (2019). Investigating the tectonic influence to

the anthropogenic subsidence along northern coast of Java Island Indonesia using GNSS data sets. E3S Web of Conferences 94, 04005. https://doi.org/10.1051/E3SCONF/20199404005

Aqil, M., Kita, I., Yano, A., Nishiyama, S., (2007). Groundwater Pump Clustering Management Strategy Using a Fuzzy C-Means Approach. Journal of Rainwater Catchment Systems 12, 17–22. https://doi.org/10.7132/JRCSA.KJ00004557610

Arifianto, I., Wibowo, R.C., (2020). Analysis of the Surface Subsidence of Porong and Surrounding Area, East Java, Indonesia based on Interferometric Satellite Aperture Radar (InSAR) Data. Journal of Geoscience, Engineering, Environment, and Technology 5, 175–180. https://doi.org/10.25299/JGEET.2020.5.4.5149

Arisbaya, I., Lestiana, H., Mukti, M.M., Handayani, L., Grandis, H., Warsa, Sumintadireja, P., (2021). Garsela Fault and other NE-SW active faults along the southern part of Java Island. IOP Conf Ser Earth Environ Sci 789, 012065. https://doi.org/10.1088/1755-1315/789/1/012065

Asdak, C., Supian, S., Subiyanto, (2018). Watershed management strategies for flood mitigation: A case study of Jakarta's flooding. Weather Clim Extrem 21, 117–122. https://doi.org/10.1016/j.wace.2018.08.002

Berardino, P., Fornaro, G., Lanari, R., Sansosti, E., (2002). A new algorithm for surface deformation monitoring based on small baseline differential SAR interferograms. IEEE Transactions on Geoscience and Remote Sensing 40, 2375–2383. https://doi.org/10.1109/TGRS.2002.803792

Chaussard, E., Amelung, F., Abidin, H., Hong, S.H., (2013). Sinking cities in Indonesia: ALOS PALSAR detects rapid subsidence due to groundwater and gas extraction. Remote Sens Environ 128, 150–161. https://doi.org/10.1016/J.RSE.2012.10.015

Chen, X., Tessari, G., Fabris, M., Achilli, V., Floris, M., (2021). Comparison Between PS and SBAS InSAR Techniques in Monitoring Shallow Landslides, in: Casagli Nicola and Tofani, V. and S.K. and B.P.T. and T.K. (Ed.), Understanding and Reducing Landslide Disaster Risk: Volume 3 Monitoring and Early Warning. Springer International Publishing, Cham, pp. 155–161. https://doi.org/10.1007/978-3-030-60311-3_17

Chrzanowski, A., Szostak-Chrzanowski, A., Bond, J., Wilkins, R., (2007). Increasing public and environmental safety through integrated monitoring and analysis of structural and ground deformations. Lecture Notes in Geoinformation and Cartography 407–426. https://doi.org/10.1007/978-3-540-72108-6_26

Cigna, F., Ramírez, R.E., Tapete, D., (2021). Accuracy of Sentinel-1 PSI and SBAS InSAR Displacement Velocities against GNSS and Geodetic Leveling Monitoring Data. Remote Sens (Basel) 13, 4800. https://doi.org/10.3390/RS13234800

Cigna, F., Tapete, D., (2021). Sentinel-1 Big Data Processing with P-SBAS InSAR in the Geohazards Exploitation Platform: An Experiment on Coastal Land Subsidence and Landslides in Italy. Remote Sens (Basel) 13, 1–26. https://doi.org/10.3390/rs13050885

Cigna, F., Tapete, D., Garduño-Monroy, V.H., Muñiz-Jauregui, J.A., García-Hernández, O.H., Jiménez-Haro, A., (2019). Wide-Area InSAR Survey of Surface Deformation in Urban Areas and Geothermal Fields in the Eastern Trans-Mexican Volcanic Belt, Mexico. Remote Sens (Basel) 11, 2341. https://doi.org/10.3390/RS11202341

Cummins, P.R., (2017). Geohazards in Indonesia: Earth science for disaster risk reduction - introduction. Geol Soc Spec Publ 441, 1–7. https://doi.org/10.1144/SP441.11/ASSET/48BE736D-0265-4063-90F3-D32A8B66D0C1/ASSETS/GRAPHIC/SP441-1992F02.JPEG

Duan, W., Zhang, H., Wang, C., Tang, Y., (2020). Multi-Temporal InSAR Parallel Processing for Sentinel-1 Large-Scale Surface Deformation Mapping. Remote Sens (Basel) 12, 3749. https://doi.org/10.3390/RS12223749

Edison, R., Rohadi, S., Perdana, Y., Riama, N.F., Karnawati, D., (2021). Seismic Vulnerability Index Calculation for Mitigation Purposes at Cilacap District. IOP Conf Ser Earth Environ Sci 873, 012005. https://doi.org/10.1088/1755-1315/873/1/012005

Fabris, M., Battaglia, M., Chen, X., Menin, A., Monego, M., & Floris, M. (2022). An Integrated InSAR and GNSS Approach to Monitor Land Subsidence in the Po River Delta (Italy). Remote Sensing 2022, Vol. 14, Page 5578, 14(21), 5578. https://doi.org/10.3390/RS14215578

Fikri, S., Anjasmara, I.M., Taufik, M., (2021). Application of Different Coherence Threshold on PS-InSAR Technique for Monitoring Deformation on the LUSI Affected Area During 2017 and 2019. IOP Conf Ser Earth Environ Sci 731, 012036. https://doi.org/10.1088/1755-1315/731/1/012036

Flament, N., Gurnis, M., Dietmar Müller, R., (2013). A review of observations and models of dynamic topography. Lithosphere 5, 189–210. https://doi.org/10.1130/L245.1

Fukushima, Y., (2023). Challenges in using Artificial Intelligence on InSAR in the Japanese context, in: AGUFM. pp. S42B-05.

Fukushima, Y., Mori, J., Hashimoto, M., Kano, Y., (2009). Subsidence associated with the LUSI mud eruption, East Java, investigated by SAR interferometry. Mar Pet Geol 26, 1740–1750. https://doi.org/10.1016/J.MARPETGEO.2009.02.001

Gagliardi, V., Tosti, F., Bianchini Ciampoli, L., Battagliere, M.L., D'Amato, L., Alani, A.M., Benedetto, A., (2023). Satellite Remote Sensing and Non-Destructive Testing Methods for Transport Infrastructure Monitoring: Advances, Challenges and Perspectives. Remote Sens (Basel) 15, 418. https://doi.org/10.3390/RS15020418

Geospatial Agency, I., (2024). Sistem Referensi Geospasial Indonesia (SRGI) [WWW Document]. URL https://srgi.big.go.id/map/jkg-active (accessed 13/01/2023).

González, P.J., Singh, K.D., Tiampo, K.F., (2015). Shallow Hydrothermal Pressurization before the 2010 Eruption of Mount Sinabung Volcano, Indonesia, Observed by use of ALOS Satellite Radar Interferometry. Pure Appl Geophys 172, 3229–3245. https://doi.org/10.1007/s00024-014-0915-7

Hadianti, A., Dewanto, B.G., (2023). The simulation of urban development with the consideration of ground deforma-

tion threats in Sidoarjo Regency, East Java Province of Indonesia. Remote Sens Appl 32, 101019. https://doi.org/10.1016/J.RSASE.2023.101019

Hakim, W.L., Fadhillah, M.F., Park, S., Pradhan, B., Won, J.-S., Lee, C.-W., (2023). InSAR time-series analysis and susceptibility mapping for land subsidence in Semarang, Indonesia using convolutional neural network and support vector regression. Remote Sens Environ 287, 113453. https://doi.org/10.1016/j.rse.2023.113453

Hamdalah, H., Wibowo, E.S., (2020). Integrate of Geoelectric and Geomagnetic Methods to Construct Subsurface Model as Early Landslides Mitigation in Kalirejo, Kokap, Kulonprogo, in: Proceeding on Engineering and Science Series (ESS). Research Synergy Foundation Press, Yogyakarta, pp. 1–11. https://doi.org/10.31098/ess.v1i1.152

Han, Y., Zhao, Y., Zhang, Y., Sarah, D., Soebowo, E., (2018). Land subsidence threats and its management in the North Coast of Java. IOP Conf Ser Earth Environ Sci 118, 012042. https://doi.org/10.1088/1755-1315/118/1/012042

Harintaka, H., Suhadha, A.G., Syetiawan, A., Ardha, M., Rarasati, A., (2024). Current land subsidence in Jakarta: a multi-track SBAS InSAR analysis during 2017–2022 using C-band SAR data. Geocarto Int 39. https://doi.org/10.1080/10106049.2024.2364726

Hayati, N., Widodo, A., Kurniawan, A., Made, D., Sanjiwani, A., Darminto, M.R., Yudha, S., Tetuko, J., Sumantyo, S., (2022). Small baselines techniques of time series InSAR to monitor and predict land subsidence causing flood vulnerability in Sidoarjo, Indonesia. Geomatics, Natural Hazards and Risk 13, 2124–2150. https://doi.org/10.1080/19475705.2022.2109518

Hong, S. H., Wdowinski, S., & Kim, S. W. (2008). Small temporal baseline subset (Stbas): A new InSAR technique for multi-temporal monitoring wetland's water level changes. International Geoscience and Remote Sensing Symposium (IGARSS), 3(1), 550–553. https://doi.org/10.1109/IGARSS.2008.4779406

Julzarika, A., (2024). Pseudo-Dynamics Identification (1817–2022) on the North Coast of Java (Pantura) using Dynamics Topography. Geodetski list 78 (101), 181–206.

Julzarika, A., Bahru, K., Terengganu, K., Town, G., Setar, A., Lumpur, K., Jaya, P., Alam, S., Bahru, J., Labuan, B., (2023). Land subsidence dynamics in Malaysia based on time-series vertical deformation using modified D-InSAR Sentinel-1. Planning Malaysia 21, 325–340. https://doi.org/10.21837/PM.V21I29.1374

Julzarika, A., Laksono, D.P., Subehi, L., Dewi, E.K., Kayat, Sofiyuddin, H.A., Nugraha, M.F.I., (2018). Comprehensive integration system of saltwater environment on Rote Island using a multidisciplinary approach. J. Degrade. Min. Land Manage 6, 1533–1567. https://doi.org/10.15243/jdmlm.2018.061.1553

Kalenjuk, S., Lienhart, W., Rebhan, M.J., (2021). Processing of mobile laser scanning data for large-scale deformation monitoring of anchored retaining structures along highways. Computer-Aided Civil and Infrastructure Engineering 36, 678–694. https://doi.org/10.1111/MICE.12656

Karadenizli, L., (2011). Oligocene to Pliocene palaeogeographic evolution of the Çankırı-Çorum Basin, central Anatolia, Turkey. Sediment Geol 237, 1–29. https://doi.org/10.1016/J.SEDGEO.2011.01.008

Kaswanto, Utami, F.N.H., (2016). The Disparity of Watershed Development between Northern and Southern Region of Java Island. Procedia Environ Sci 33, 21–26. https://doi.org/10.1016/J.PROENV.2016.03.052

Kavzoglu, T., Sen, Y.E., Cetin, M., (2009). Mapping urban road infrastructure using remotely sensed images. Int J Remote Sens 30, 1759–1769. https://doi.org/10.1080/01431160802639582

Khakim, M.Y.N., Supardi, S., Tsuji, T., (2023). Earthquake affects subsidence in Jakarta using Sentinel-1A time series images and 2D-MSBAS method. Vietnam Journal of Earth Sciences 45, 111–130. https://doi.org/10.15625/2615-9783/18021

Khakim, M.Y.N., Tsuji, T., Matsuoka, T., (2013). Monitoring and characterization of land subsidence in the Bandung Basin, West Java, Indonesia using SAR interferometry. SEG Technical Program Expanded Abstracts 32, 4960–4965. https://doi.org/10.1190/segam2013-0221.1

Koulali, A., McClusky, S., Susilo, S., Leonard, Y., Cummins, P., Tregoning, P., Meilano, I., Efendi, J., Wijanarto, A.B., (2017). The kinematics of crustal deformation in Java from GPS observations: Implications for fault slip partitioning. Earth Planet Sci Lett 458, 69–79. https://doi.org/10.1016/J.EPSL.2016.10.039

Kralj, P., (2012). Facies architecture of the Upper Oligocene submarine Smrekovec stratovolcano, Northern Slovenia. Journal of Volcanology and Geothermal Research 247–248, 122–138. https://doi.org/10.1016/J.JVOLGEORES.2012.07.016

Kumazawa, S., (1994). Quaternary geology and hydrogeology of the Madiun. Journal of geosciences Osaka City University 37, 213–242.

Kurnio, H., (2007). Review of Coastal Characteristics of Iron Sand Deposits in Cilacap Central Java. Bulletin of the Marine Geology 22, 35–49. https://doi.org/10.32693/bomg.v22i1.4

Lanari, R., Mora, O., Manunta, M., Mallorquí, J.J., Berardino, P., Sansosti, E., (2004). A small-baseline approach for investigating deformations on full-resolution differential SAR interferograms. IEEE Transactions on Geoscience and Remote Sensing 42, 1377–1386. https://doi.org/10.1109/TGRS.2004.828196

Li, S., Xu, W., Li, Z., (2022). Review of the SBAS InSAR Time-series algorithms, applications, and challenges. Geod Geodyn 13, 114–126. https://doi.org/10.1016/j.geog.2021.09.007

Li, Y., Ji, P., Liu, S., Zhao, J., Yang, Y., (2024). Susceptibility evaluation of highway landslide disasters based on SBAS-InSAR: a case study of S211 highway in Lanping County. Natural Hazards 1–26. https://doi.org/10.1007/s11069-024-06807-7

Liu, N., Dai, W., Santerre, R., Hu, J., Shi, Q., & Yang, C. (2019). High Spatio-Temporal Resolution Deformation Time Series with the Fusion of InSAR and GNSS Data Using Spatio-Temporal Random Effect Model. IEEE Transactions on Geoscience and Remote Sensing, 57(1), 364–680. https://doi.org/10.1109/TGRS.2018.2854736

Lubis, A.M., Sato, T., Tomiyama, N., Isezaki, N., Yamanokuchi, T., (2011). Ground subsidence in Semarang-Indonesia investigated by ALOS–PALSAR satellite SAR interferometry. J Asian Earth Sci 40, 1079–1088. https://doi.org/10.1016/J.JSEAES.2010.12.001

Luo, Q., Li, J., Zhang, Y., (2022). Monitoring Subsidence over the Planned Jakarta–Bandung (Indonesia) High-Speed Railway Using Sentinel-1 Multi-Temporal InSAR Data. Remote Sens (Basel) 14. https://doi.org/10.3390/rs14174138

Malawani, M.N., Mardiatno, D., Haryono, E., (2020). Anthropogenic Signatures in the Context of Landscape Evolution: Evidence from Citanduy Watershed, Java, Indonesia. ASEAN Journal on Science and Technology for Development 37, 3. https://doi.org/10.29037/ajstd.600

Marsella, M., Scaioni, M., (2018). Sensors for Deformation Monitoring of Large Civil Infrastructures. Sensors 18, 3941. https://doi.org/10.3390/S18113941

Meng, X., Roberts, G.W., Dodson, A.H., Cosser, E., Barnes, J., Rizos, C., (2004). Impact of GPS satellite and pseudolite geometry on structural deformation monitoring: Analytical and empirical studies. J Geod 77, 809–822. https://doi.org/10.1007/s00190-003-0357-y

Morishita, Y., Lazecky, M., Wright, T.J., Weiss, J.R., Elliott, J.R., Hooper, A., (2020). LiCSBAS: An Open-Source InSAR Time Series Analysis Package Integrated with the LiCSAR Automated Sentinel-1 InSAR Processor. Remote Sensin 12, 424. https://doi.org/10.3390/RS12030424

Morishita, Y., Sugimoto, R., Nakamura, R., Tsutsumi, C., Natsuaki, R., Shimada, M., (2023). Nationwide urban ground deformation in Japan for 15 years detected by ALOS and Sentinel-1. Progress in Earth and Planetary Science 2023 10:1 10, 1–20. https://doi.org/10.1186/S40645-023-00597-5

Motohka, T., Kankaku, Y., Miura, S., & Suzuki, S. (2019). Alos-4 L-Band SAR Mission and Observation. International Geoscience and Remote Sensing Symposium (IGARSS), 5271–5273. https://doi.org/10.1109/IGARSS.2019.8898169

Negara, L.P., Lestari, D., Kurnianto, F.A., Ikhsan, F.A., Apriyanto, B., Nurdin, E.A., (2021). An overview of depositional environment between the mountains of southern java and the fold mountain of north java. IOP Conf Ser Earth Environ Sci 683, 012005. https://doi.org/10.1088/1755-1315/683/1/012005

Nelson, D.A., Cottle, J.M., (2017). Long-Term Geochemical and Geodynamic Segmentation of the Paleo-Pacific Margin of Gondwana: Insight From the Antarctic and Adjacent Sectors. Tectonics 36, 3229–3247. https://doi.org/10.1002/2017TC004611

Noufal, A., Shebl, H., (2019). Halokinesis Stimuluses on Petroleum System of Abu Dhabi. Society of Petroleum Engineers - Abu Dhabi International Petroleum Exhibition and Conference 2019, ADIP 2019. https://doi.org/10.2118/197597-MS

Nugraha, S., Alfahmi, S., Wiwit, H., Cahyono, H., Penelitian, P., Hidup, L., (2023). Analisis Pola Aliran dan Kuantitas Air Tanah Dangkal di Kota Madiun. ENVIRO: Journal of Tropical Environmental Research 25, 52–65. https://doi.org/10.20961/ENVIRO.V25I1.78749

Nugrahaeni, S.B., Purnama, I.L.S., Primacintya, V.A., (2021). Evaluation of groundwater usage in relationship to groundwater vulnerability to sea water intrusion in Cilacap Coastal. E3S Web of Conferences 325, 08004. https://doi.org/10.1051/E3SCONF/202132508004

Pasari, S., Simanjuntak, A.V.H., Mehta, A., Neha, Sharma, Y., (2021). The Current State of Earthquake Potential on Java Island, Indonesia. Pure Appl Geophys 178, 2789–2806. https://doi.org/10.1007/s00024-021-02781-4

Pepe, A., Calò, F., (2017). A Review of Interferometric Synthetic Aperture RADAR (InSAR) Multi-Track Approaches for the Retrieval of Earth's Surface Displacements. Applied Sciences 7, 1264. https://doi.org/10.3390/APP7121264

Pomar, L., Esteban, M., Martinez, W., Espino, D., Castillo de Ott, V., Benkovics, L., & Castro Leyva, T. (2015). Oligocene–Miocene carbonates of the Perla Field, offshore Venezuela: Depositional model and facies architecture. In American Association of Petroleum Geologists Bulletin (Vol. 91, pp. 647–673). https://doi.org/10.1306/10160606043

Pribadi, A., (2019). Pemanfaatan Air Tanah Harus Memperhatikan Keseimbangan Lingkungan. Minister of Energy and Mineral Resources. https://www.esdm.go.id/id/media-center/arsip-berita/pemanfaatan-air-tanah-harus-memperhatikan-keseimbangan-lingkungan. (accessed 24/02/2025)

Purnama, S., (2019). Groundwater Vulnerability from Sea Water Intrusion in Coastal Area Cilacap, Indonesia. Indonesian Journal of Geography 51, 206–216. https://doi.org/10.22146/IJG.18229

Raspini, F., Caleca, F., Del Soldato, M., Festa, D., Confuorto, P., Bianchini, S., (2022). Review of satellite radar interferometry for subsidence analysis. Earth Sci Rev 235, 104239. https://doi.org/10.1016/J.EARSCIREV.2022.104239

Rizos Chris, Han, S., Craigand, R., Han, X., aAbidin, H.Z., Suganda, O.K., Wirakusumah, A.D., (2000). Continuously operating GPS-based volcano deformation monitoring in Indonesia: the technical and logistical challenges, in: Schwarz, K.-P. (Ed.), Geodesy Beyond 2000. Springer Berlin Heidelberg, Berlin, Heidelberg, pp. 361–366. https://doi.org/10.1007/978-3-642-59742-8_59

Root, B.C., Van Der Wal, W., Novák, P., Ebbing, J., Vermeersen, L.L.A., (2015). Glacial isostatic adjustment in the static gravity field of Fennoscandia. J Geophys Res Solid Earth120,503–518.https://doi.org/10.1002/2014JB011508

Rosen, P., Hensley, S., Shaffer, S., Edelstein, W., Kim, Y., Kumar, R., Misra, T., Bhan, R., Satish, R., & Sagi, R. (2016). An update on the NASA-ISRO dual-frequency DBF SAR (NISAR) mission. International Geoscience and Remote Sensing Symposium (IGARSS), 2016-November, 2106–2108. https://doi.org/10.1109/IGARSS.2016.7729543

Sarah, D., (2022). Land subsidence hazard in Indonesia: Present research and challenges ahead. RISET Geologi dan Pertambangan 32, 83. https://doi.org/10.14203/risetgeotam2022.v32.1195

Sarah, D., Soebowo, E., Sudrajat, Y., Satriyo, N.A., Putra, M.H.Z., Wahyudin, (2023). Mapping the environmental impacts from land subsidence hazard in Pekalongan City and its correlation with the subsurface condition. IOP Conf Ser Earth Environ Sci 1201, 012044. https://doi.org/10.1088/1755-1315/1201/1/012044

Saroso, H.W., (1988). Natural slope problems related to roads in Java, Indonesia, in: Proc 2nd International Conference on Geomechanics in Tropical Soils, Singapore. Rotterdam, pp. 259–266. https://doi.org/10.1016/0148-9062(90)90398-L

Satyana, A.H., Erwanto, E., Prasetyadi, C., (2004). Rembang-Madura-Kangean-Sakala (RMKS) Fault Zone, East Java Basin: The Origin and Nature of a Geologic Border, in: Indonesian Association of Geologists 33rd Annual Convention. Bandung.

Sidiq, T.P., Gumilar, I., Meilano, I., Abidin, H.Z., Andreas, H., Permana, A., (2021). Land Subsidence of Java North Coast Observed by SAR Interferometry. IOP Conf Ser Earth Environ Sci 873, 012078. https://doi.org/10.1088/1755-1315/873/1/012078

Smyth, H.R., Hall, R., Nichols, G.J., (2008). Cenozoic volcanic arc history of East Java, Indonesia: The stratigraphic record of eruptions on an active continental margin. Special Paper of the Geological Society of America 436, 199–222. https://doi.org/10.1130/2008.2436(10)

Soeria-Atmadja, R., Maury, R.C., Bellon, H., Pringgoprawiro, H., Polve, M., Priadi, B., (1994). Tertiary magmatic belts in Java. J Southeast Asian Earth Sci 9, 13–27. https://doi.org/10.1016/0743-9547(94)90062-0

Solihuddin, T., Husrin, S., Mustikasari, E., Heriati, A., Kepel, T.L., Salim, H.L., Risandi, J., Dwiyanti, D., (2021a). Coastal Inundation and Land Subsidence in North Coast of West Java: A New Hazard? IOP Conf Ser Earth Environ Sci 925, 012015. https://doi.org/10.1088/1755-1315/925/1/012015

Solihuddin, T., Husrin, S., Salim, H.L., Kepel, T.L., Mustikasari, E., Heriati, A., Ati, R.N.A., Purbani, D., Mbay, L.O.N., Indriasari, V.Y., Berliana, B., (2021b). Coastal erosion on the north coast of Java: adaptation strategies and coastal management. IOP Conf Ser Earth Environ Sci 777, 012035. https://doi.org/10.1088/1755-1315/777/1/012035

Sudarsono, U., Sudjarwo, I.B., 2008. Amblesan di daerah Porong, Kabupaten Sidoarjo, Jawa Timur. Indonesian Journal on Geoscience 3, 1–9. https://doi.org/10.17014/IJOG.3.1.1-9

Suhadha, A.G., Chusnayah, F., Julzarika, A., (2023a). Seismic-Induced Displacement Dynamics in Banten's Irrigation Zones: DInSAR Monitoring (2017–2020). Doklady Earth Sciences. https://doi.org/10.1134/S1028334X23602444

Suhadha, A.G., Harintaka, (2023). Assessing Three-Dimensional Displacement in the Low Latitude Area from Multi-Geometry Sentinel-1 InSAR: Case Study Palu City, in: APSAR 2023 - 2023 8th Asia-Pacific Conference on Synthetic Aperture Radar. Institute of Electrical and Electronics Engineers Inc. https://doi.org/10.1109/APSAR58496.2023.10389130

Suhadha, A.G., Harintaka, H., (2024). Multidimensional displacement analysis of Semeru Volcano, Indonesia following December 2021 eruption from multitrack InSAR observation. Earth Sci Inform. https://doi.org/10.1007/s12145-024-01248-z

Suhadha, A.G., Julzarika, A., (2022). Dynamic Displacement using DInSAR of Sentinel-1 in Sunda Strait. Trends in Sciences 19, 4623. https://doi.org/10.48048/tis.2022.4623

Suhadha, A.G., Julzarika, A., Ardha, M., Chusnayah, F., (2021). Monitoring Vertical Deformations of the Coastal City of Palu after Earthquake 2018 Using Parallel-SBAS, in: 2021 7th Asia-Pacific Conference on Synthetic Aperture Radar, APSAR 2021. Institute of Electrical and Electronics Engineers Inc., Bali, Indonesia. https://doi.org/10.1109/APSAR52370.2021.9688380

Suhadha, A.G., Julzarika, A., Susilo, S., Meilano, I., Syetiawan, A., Ramdani, D., (2023b). Identification of tectonic activity of the Baribis fault revealed by present Sentinel-1 InSAR observation. Jakarta, Indonesia, p. 030010. https://doi.org/10.1063/5.0181387

Suhadha, A.G., Prayoga, O., Harintaka, (2023c). Precise coseismic displacement related to the 2022 Pasaman earthquake using multi-geometry of Sentinel-1 InSAR. Jakarta, Indonesia, p. 030008. https://doi.org/10.1063/5.0181385

Supendi, P., Nugraha, A.D., Puspito, N.T., Widiyantoro, S., Daryono, D., (2018). Identification of active faults in West Java, Indonesia, based on earthquake hypocenter determination, relocation, and focal mechanism analysis. Geosci Lett 5, 1–10. https://doi.org/10.1186/s40562-018-0130-y

Susilo, A., Sunaryo, S., Suryo, A., Rachmawati, T., Sutasoma, M., (2021). Analysis of Landslide and Land Subsident Using Geophysical Method in the East Java Province, Indonesia, in: Zhang, Y., Cheng, Q. (Eds.), Landslides. IntechOpen. https://doi.org/http://dx.doi.org/10.5772/intechopen.100160

Susilo, S., Meilano, I., Wibowo, S.T., Syetiawan, A., Gaol, Y.A.L., Ramdani, D., Julzarika, A., (2022). Geodetic Strain of the Baribis Fault Zone in West Java, Indonesia. IOP Conf Ser Earth Environ Sci 1109, 012008. https://doi.org/10.1088/1755-1315/1109/1/012008

Susilo, S., Salman, R., Hermawan, W., Widyaningrum, R., Wibowo, S.T., Lumban-Gaol, Y.A., Meilano, I., Yun, S.-H., (2023). GNSS land subsidence observations along the northern coastline of Java, Indonesia. Sci Data 10, 1–8. https://doi.org/10.1038/s41597-023-02274-0

Takagi, H., CAO, V.Q.A., Esteban, M., (2023). Cumulative Land Subsidence in Populated Asian Coastal Cities. Journal of Coastal and Riverine Flood Risk 1. https://doi.org/10.59490/JCRFR.2023.0002

Takagi, H., Esteban, M., Mikami, T., Fujii, D., Kurobe, S., (2016). Mechanisms of Coastal Floods in Jakarta: The Need for Immediate Action Against Land Subsidence. The 12th International Conference on Coasts 6–7.

Thamer, Z.K., Hamdullah, A.H., Mohammed, M.U., Sowgath, M.T., (2023). The Utility of LiCSBAS to Carry out InSAR Time Series to Analyze Surface Deformation: An Overview. Journal of Techniques 5, 41–45. https://doi.org/10.51173/JT.V5I4.1639

Turcotte, D., Schubert, G., (2014). Geodynamics, 3rd ed. Cambridge University Press, Cambridge. https://doi.org/10.1017/CBO9780511843877

Verstappen, H.Th., (2010). Indonesian Landforms and Plate Tectonics. Indonesian Journal on Geoscience 5, 197–207. https://doi.org/10.17014/IJOG.5.3.197-207

Whitford, D.J., Nicholls, I.A., Taylor, S.R., (1979). Spatial variations in the geochemistry of quaternary lavas across the Sunda arc in Java and Bali. Contributions to Mineral-

ogy and Petrology 70, 341–356. https://doi.org/10.1007/BF00375361

Widiatmoko, F.R., Sari, A.S., Ramadhanty, J.A.N., Putri, R.H.K., (2021). Study of Hydrothermal Alteration and Mineralization in the Lahbako Field, Jember Regency, East Java Province. J Phys Conf Ser 2117, 012004. https://doi.org/10.1088/1742-6596/2117/1/012004

Widiyantoro, S., Gunawan, E., Muhari, A., Rawlinson, N., Mori, J., Hanifa, N.R., Susilo, S., Supendi, P., Shiddiqi, H.A., Nugraha, A.D., Putra, H.E., (2020). Implications for megathrust earthquakes and tsunamis from seismic gaps south of Java Indonesia. Sci Rep 10. https://doi.org/10.1038/s41598-020-72142-z

Yong, L., Long, Z., Lin, Z., Fang, T., Kunchao, L., Aihua, S., (2020). Land subsidence characteristics and disaster prevention in the Tongzhou area, Beijing. Proceedings of the International Association of Hydrological Sciences 382, 715–719. https://doi.org/10.5194/PIAHS-382-715-2020

Yulyta, S.A., Taufik, M., Hayati, N., (2016). Land subsidence detection using synthetic aperture radar (SAR) in Sidoarjo Mudflow area. AIP Conf Proc 1730. https://doi.org/10.1063/1.4947408/884613

Zaenal Putra, M.H., Suhadha, A.G., Hermawan, W., Sarah, D., Handika, R., Soebowo, E., Satriyo, N.A., (2024). Assessing Regional Surface Subsidence and Its Impact on Critical Infrastructure in Gedebage, Bandung Using SBAS InSAR Analysis, in: 2024 IEEE International Conference on Aerospace Electronics and Remote Sensing Technology (ICARES). IEEE, pp. 1–6. https://doi.org/10.1109/ICARES64249.2024.10767940

Zaenudin, A., Darmawan, I.G.B., Armijon, Minardi, S., Haerudin, N., (2018). Land subsidence analysis in Bandar Lampung City based on InSAR, in: Journal of Physics: Conference Series. Institute of Physics Publishing. https://doi.org/10.1088/1742-6596/1080/1/012043

SAŽETAK

Redefiniranje žarišnih područja slijeganja i izdizanja tla na otoku Javi, Indonezija: viševremenska InSAR analiza za kartiranje deformacija tla velikih razmjera

Otok Java doživljava složene i nelinearne deformacije tla uzrokovane interakcijom prirodnih i antropogenih čimbenika. Dosadašnja istraživanja uglavnom su bila usmjerena na slijeganje tla u urbanim sredinama ostavljajući obrasce deformacija na razini cijeloga otoka nedovoljno istraženima. Ovo istraživanje rješava taj nedostatak korištenjem viševremenske interferometrije sintetičkoga radara s otvorom antene (engl. *Multi-Temporal Interferometric Synthetic Aperture Radar,* MT-InSAR), kojom se identificiraju opsežni obrasci slijeganja i izdizanja tla na čitavome otoku Java. Rezultati pokazuju prethodno nedovoljno istraženo slijeganje tla u Karawangu (–1795 mm), Cilacapu (–902 mm) i Madiunu (–742 mm), koje premašuje slijeganje u priobalnome području Jakarte. Važno je istaknuti da se najizraženije slijeganje na području Velike Jakarte odvija u unutrašnjosti, kod Bekasija i Cikaranga, čime se osporavaju tradicionalne pretpostavke o slijeganju u urbanim zonama te pruža šire razumijevanje regionalne geodinamike otoka Java. Integracijom analize žarišnih područja i MT-InSAR metodologije unapređuje se praćenje deformacija tla te se naglašava važnost kontinuiranoga monitoringa za učinkovito upravljanje zemljištem i planiranje infrastrukture, posebice u visokorizičnim područjima koja nisu dovoljno pokrivena mjerenjima, kao što su Karawang, Cilacap i Madiun. Dobiveni rezultati mogu se primijeniti u geološkim istraživanjima, urbanističkome planiranju te donošenju politika u svrhu ublažavanja geoloških opasnosti i osiguravanja održivoga razvoja.

Ključne riječi:
InSAR, vertikalni pomak tla, LiCSBAS, slijeganje tla, Sentinel-1

Author's contribution

Argo Galih Suhadha: conceptualization, data curation, methodology, validation, visualization, writing-original manuscript, writing-review, and editing, **Mohammad Ardha**: data processing, writing-original manuscript, and visualization, **Farikhotul Chusnayah:** writing-original manuscript, writing-review, and editing**, Rido Dwi Ismanto**: writing-original manuscript, writing-review, and editing**, Rizky Ahmad Yudanegara:** writing-review, and editing**, Atriyon Julzarika:** methodology, manuscript writing-review & editing, and supervising the work.
All authors have read and agreed to the published version of the manuscript.